POLITECNICO DI TORINO

Facoltà di Ingegneria

Corso di Laurea Magistrale in Ingegneria Energetica e Nucleare

Tesi di Laurea Magistrale

NON-THERMAL PLASMA ASSISTED CO_2 SPLITTING: PARAMETRIC PLASMA TORCH STUDY WITH INERT GASSES

Candidato:
Alberto Ferrari

Relatori:
Prof. Massimo Santarelli
CO-Relatori:
Prof. Domenico Ferrero
PhD Francesco Orsini
PhD Salvatore Francesco Cannone
Domenico D'Angelo

26 November 2024

Contents

Abstract

The topic of Carbon Dioxide(CO_2) emissions is currently very debated, mainly because of the environmental impact in terms of atmosphere pollution, greenhouse gas effect, and climate change. Several approaches are being considered to fight the climate change and to mitigate CO_2 emissions, such as carbon capture and storage (CCS), utilization (CCU), and catalytic CO_2 conversion. In this framework, a promising technology is the plasma assisted CO_2 conversion, which is able to convert CO_2 into useful products such as carbon monoxide (CO) and oxygen (O_2) at ambient conditions and with a low energy consumption. This technology could sustain the CO_2 management and lead to the creation of a sustainable carbon economy. Research is ongoing to optimize the process. This thesis proposes a preliminary experimental evaluation of the plasma-assisted CO_2 splitting reaction making use of a test bench currently under development in our laboratories, together with a wide literature overview of the process. The test bench comprises an arc plasma system (Plasmatreat GmbH) consisting of a generator (FG5001), a Power Control Unit (range from 400 to 600W) and a source (Openair-Plasma PFW10). The plasma parameters were set via an interface designed to appropriately handle both the electrical parameters (electric voltage and frequency) and the gas volumes fed into the system. An Ocean Optics LIBS2500 Plus spectrometer (Ocean Optics, Inc., Dunedin, FL, USA), a fiber optic cable and the OceanView computer software (OceanView version 2.0.8) were used to examine the spectra of the species in the sensitive range from 150 to 1100 nm as wavelength. The probe was positioned in proximity to the plasma jet so that it operated in an overpressure environment. This condition provides an indication of the capacity of the plasma flow without any influence from the air surrounding the treatment chamber: the OES shows the potential ionizing effect of the chemical species involved and their variation with the primary plasma parameters. This provides preliminary guidance on the choice of parameters to adopt in combination with preliminary experiments.

1 Overview on the Plasma technology

Plasma is usually referred to as the "fourth state of the matter". It is an ionized gas, meaning that it is composed of ions, unbound electrons, and neutral particles [1]. The ionization degree in the plasma can vary ranging from fully ionized gasses to a partially ionized gasses [2]. In addition, all the species that are present in the ionized gas interact among each other, thereby leading to a mixture that can be highly reactive and can be interesting in many applications purposes. Plasma can be already found in different biomedical applications, surface modification technologies, agriculture, microelectronics, or laser applications.

1.1 Plasma technologies

Plasma can be classified as natural plasma, high temperature plasma, and weakly ionized plasma. Natural plasma is basically all the matter that composes the universe and is mainly attributed to the interstellar matter and stars. High temperature plasma occurs in the fusion reactors, where the gas is typically completely ionized. Weakly ionized plasma includes all the typologies of plasma that can be generated in laboratory environment for different purposes, and that could have a large range of ionization of the gas. A second subdivision can be done focusing on whether the plasma is in thermal equilibrium or not. Indeed, the temperature has a crucial role in the plasma formation, since it is determined by the average energies of the different species and their relevant degrees of freedom such as translational, rotational and electronic. This means that when temperature in a restricted area is uniform, the plasma is said to be in local thermodynamic equilibrium (LTE), or is also referred to as thermal plasma. Instead, when the temperature is not uniform in the given area, the plasma is said to be in non-local thermodynamic equilibrium (non-LTE), or is also referred to as non-thermal plasma [2]. Thermal plasmas can be formed in two different ways: either by achieving high temperature (from 4000 K to 20000 K), or at high gas pressure. The latter can be performed in the following way: first of all, the electrons receive energy from the electric field, and lose part of that energy during collisions with the so-called heavy particles. Then, the continuing collision between particles leads to a temperature changing up to the equilibrium between the electron and heavy particle temperature. The high pressure can guarantee that more collisions occur, so a large energy efficiency exchange is reached. The main advantages of this plasma typology are that it can work at high temperature, high non-ionizing radiation, and high energy density. This means that thermal plasma, and particularly the heat source, can be directional,

with a sharp interference and a thermal gradient that is controlled independently from the chemistry. This make it particularly convenience in the case of coating technologies, fine powder synthesis and treatment of waste materials. Non-thermal plasma is obtained by applying a differential in electric potential between two parallel electrodes, which are placed inside a reactor filled with gas or they form the reactor walls. A gas breakdown is obtained by the potential difference with the result of positive ions and electrons. In particular, the electrons are accelerated by the electric field towards the anode. When the electrons collide with gas molecules it generates:

- The ionization collision which is a fundamental process in plasma, referring to the conversion of neutral atoms or molecules into electrons and positive ions. As such, ionization represents the primary elementary chemical process to consider in plasma phenomena.

- The excitation collisions create excited molecules that can decay in the ground state and emit light.

- The dissociation process creates radicals that can form new compounds, being this the basis of gas conversion applications of non-thermal plasma. In non-thermal plasma, the electrons are characterized by a much higher temperature than the heavy particles. In general the electron temperature is of the order of 1 eV ($\sim 10000K$), while the gas temperature remains close to the room temperature. The high electron temperature is due to the small mass of the electrons that are accelerated by the electric field, against the heavy particles that are not accelerated. As a consequence, the heavy particle, having a larger mass, will lose more energy during the elastic collision, instead of the small particle that can gain the energy from the electric field.

Finally, the major advantage of this type of plasma is that allows gases, even unreactive gases, to be activated at room temperature by the highly energetic electrons. Thus, heating the entire reactor is not needed. Instead, an electromagnetic field is necessary. This means high flexibility, since it can be easily turned off and on, and the power consumption can easily be scaled and adjusted [2]. Warm plasma is identified as a transition type of plasma. Indeed, it operates at boundary conditions of thermal and non-thermal plasmas. The key point of this technology is that it is able to create the advantage of non-equilibrium conditions, while at the same time operating at higher temperature. In that case, the non-equilibrium conditions, typical of non-thermal plasmas, allow for more

efficient chemical reactions due to the presence of high-energy electrons that interact with atoms or molecules without the need for high temperatures throughout the system. Warm plasma can leverages this characteristic and offers higher temperatures, which improve particle density and ionization. This promotes faster and more complete chemical reactions, increasing process efficiency, which is beneficial in many industrial processes such as CO_2 conversion, material synthesis, or chemical activation [3]. In practice, warm plasma is able to combine the benefits of a low gas temperature, typical of non-thermal plasmas, with the ability of high temperatures, characteristic of thermal plasmas, to generate more intense and controllable reactions. This makes it ideal for applications that require both high electron energy and relatively low temperatures, optimizing energy efficiency without waste [2]. Non-thermal plasma has been object of increasing interest in recent years. The most common types of plasma technologies reported in the literature for the CO_2 splitting are dielectric barrier discharge (DBD), microwave (MW), gliding arc (GA), and plasma torch [4]. Non-thermal plasma is widely used for surface treatment and material modifications, such as improving adhesion and wear resistance of materials like metals, plastics, and textiles. Its ability to modify surfaces without significantly heating the material makes it ideal for delicate treatments, such as in polymer processing [3]. Additionally, non-thermal plasma plays a key role in the decomposition and conversion of gases, including CO_2 conversion into valuable products like CO and oxygen. Microwave plasma and plasma torches are commonly employed for such processes. The technology is also used for environmental applications like air and water purification, where it helps remove pollutants without using harmful chemicals. Non-thermal plasma also finds applications in the synthesis of advanced materials, such as nanoparticles, and in semiconductor manufacturing for processes like etching and thin-film deposition [3].Overall, non-thermal plasma stands out for its ability to provide high-energy electron interactions while keeping the gas temperature relatively low, making it ideal for applications that require precise control over chemical reactions and material treatments.

1.1.1 DBD

DBD is the most used type of plasma technology that has been known for many years. DBD is used in various applications, including surface treatment, pollution control, ozone generation and synthesis of fuel or chemical[5]. It consists of two parallel electrodes that contain a dielectric barrier (*e.g.* glass, quartz, ceramic material, or polymers [6]). In this dielectric material, a small, limited alternating current can pass, generating the discharge

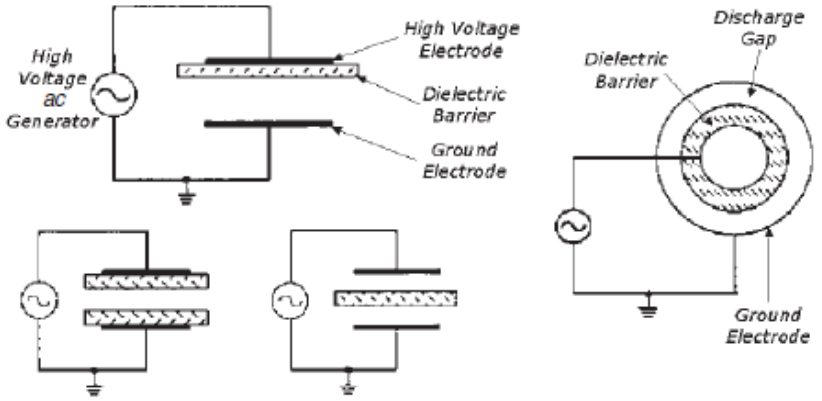

Figure 1: Common DBD configuration: planar and cylindrical [7]

in only one direction. So, to transport the current in the discharge gap, an electric field is required to cause the breakdown in the gas. The role of the dielectric material is to be an insulator between the two electrodes, thereby limiting the electric current and blocking the spark formation [2]. The typical configurations of DBDs are illustrated in Fig. 1, in which a gas flow is applied in the gap, this latter varying typically from 0.1 mm up to several cm [7]. Generally, DBDs operate also at approximately atmospheric pressure (0.1-10 atm), while alternating the voltage with an amplitude of 1-100 kV, and a frequency of a few Hz to MHz is applied in both electrodes [2]. As reported before, DBDs are now used for a wide range of applications, making it easier to build different geometries for the specific purpose [8].

1.1.2 MicroWave

Microwave plasma belongs to the groups of warm plasmas. The electrode is not present and the electric power is applied by microwaves. As can be seen from Fig.2, a MW plasma reactor is made of a quartz tube, inserted into a microwave cavity, powered by a microwave generator with a frequency of few GHz. When the MW power is introduced through the wave guide into the cavity, the gas flowing through the quartz tube is excited to form plasma [9]. MW discharges is already used for scientific, medical, and industrial applications such as nanotubes and advanced materials [8]. In those cases several types of MW have been projected, like surface wave discharges, electron cyclotron resonance and cavity induced discharges. The former (surface wave discharge) is commonly used for the conversion of the (CO_2) [10]. In particular, the electrons produced with this type of plasma are able to populate the low energy vibrational level of (CO_2), thereby enhancing the vibrational pathway for the dissociation [9].

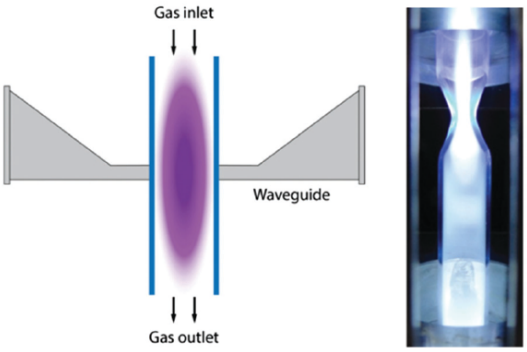

Figure 2: Schematic and image of a MW discharge [9]

1.1.3 Gliding Arc

GA discharge belongs to the category of warm plasmas, so it combine both the characteristics of the thermal and non-thermal systems [7]. A classical GA plasma configuration is represented in Fig.3, where the gas flows between two diverging electrodes. When a potential difference is applied between the two electrodes, a plasma arc is formed in the narrowest part, which is transported by the gas flow towards a rising interelectrode distance, until it becomes smoother and a new arc is ignited in the tightest part [2]. In

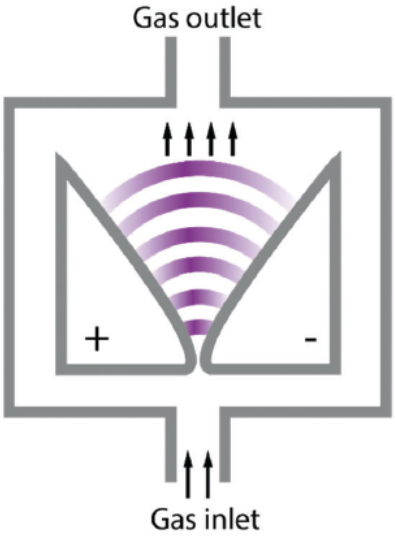

Figure 3: schematic of a GA [2].

general, the GA plasma is weakly ionized and the energy of the electrons is noticeably higher than that of the heavy species. Indeed, it has been reported that the electron temperature in the non-equilibrium region is around 11600 K, whereas vibrational and translational temperatures are around 2000-3000 K and 800-2100 K [8]. Furthermore, during the cycle of plasma formation, the GA dissipates 70-80% of the energy in the non-local

thermodynamic zone, hence the energy utilization rate is quite high [11]. Nonetheless, this type of plasma has some limits, such as the electrode geometry, the non-uniform gas conversion, and the high gas flow rate that is needed to drag the arc [2]. It presents a good efficiency of GA discharges in applications such as advanced oxidation techniques [8], environmental applications [12], material processing [13], and medical science [14].

1.1.4 Plasma jet

Plasma jet consist of two concentric electrodes through which a mixture of gasses flows. By applying a frequency at a certain voltage, the gas discharge is ignited. The ionized gas from the plasma jet exits through a nozzle, where it is directed onto a substrate a few millimeters downstream [15]. The electron flux exhibits high velocity and is hot.

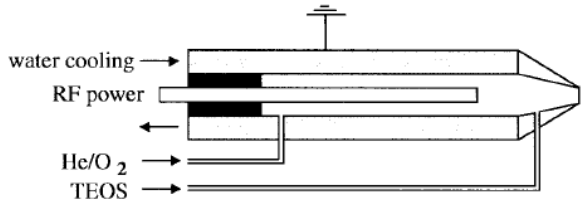

Figure 4: Schematic of the atmospheric pressure plasma jet[15].

These fast electrons excite or ionize atoms and molecules of a feed gas, such as argon. Argon ions, on the other hand, are heavier than electrons and thus are less affected by the electric field, preventing their acceleration. Additionally, fast electrons inefficiently transfer their energy to the heavy particles, which consequently remain cold. Since the temperature of a gas's heavy particles determines its overall temperature, the plasma contains highly energized particles without showing the significant temperature increase that would usually accompany them (non-equilibrium plasma) [16].

1.2 Plasma catalysis

Plasma catalysis is a new emerging branch of plasma processing, lying at the interface of various disciplines. The aim of this approach is to enhance the plasma reaction by adding a catalyst to the reaction cycle and vice versa. Combining plasma with a catalytic material is favorable for the inert molecules that are activated and then the activated species recombine at the catalytic surface to yield the desired products [2]. In particular, plasma and catalysis can be combined in two main configuration that are shown in Fig.5. The former configuration (Fig.5(a)) is a single stage process, in which the catalyst, that

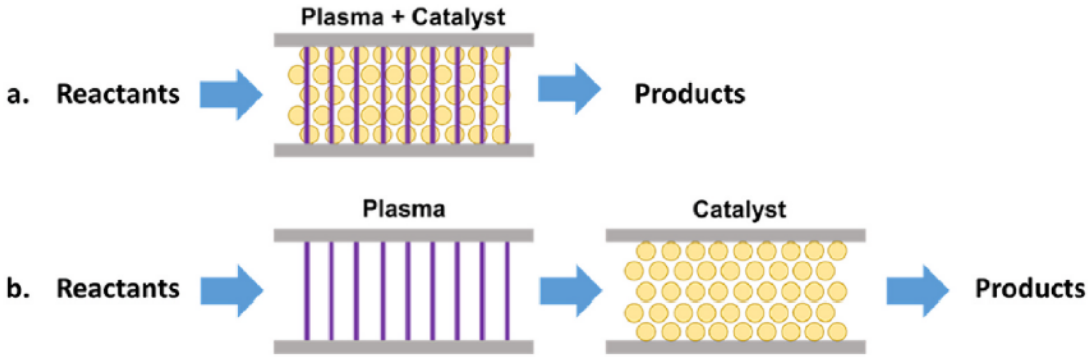

Figure 5: Schematic of different plasma catalysis configuration: a) in-plasma catalysis b) post-plasma catalysis[11].

could be partially or fully packed, is situated in the discharge region of the plasma. With this set up, the short- and long-lived reactive species can interact directly with the catalyst surface in the plasma zone, thereby increasing the conversion of the reactants to the desirable products. This can help to improve the efficiency of the process as the energy required to generate the short-lived species is often wasted. The in-plasma catalysis is mostly used for CO_2 by improving the selectivity of the target product [11]. On the contrary, post-plasma catalysis (Fig.5(b)), is a two stage process. Specifically, in the first stage, the reactants undergo to plasma gas phase reactions, while in the second stage they undergo to catalytic surface reactions. So, as the catalyst is placed downstream of the discharge zone, the vibrational excited species, which are short-lived species, cannot survive from the discharge zone to the catalyst bed, and only the long-lived species produced in the plasma will interact with the catalyst surface [17]. Generally the configuration with the catalyst downstream is mostly used, mainly due to the low thermal stability of the catalyst [2].

2 Plasma technology for CO_2 conversion

This section reports specifically on literature investigations concerning the CO_2 plasma conversion reaction. In particular, an overview of the characteristic of the pure CO_2 and the main ways in which it is dissociated are presented. Furthermore, the efficiency parameters are introduced and illustrated with a comparison among all the main plasma technologies already tested.

2.1 Overview of CO_2 conversion

The decomposition of CO_2 is the initial step for the CO_2 utilization process. Carbon monoxide (CO) and oxygen (O_2) are the main products in a theoretical splitting . However, the reaction of decomposition of CO_2 is not theoretical and several other compounds could be present, making the total decomposition more difficult to achieve.

2.1.1 Characteristic pure thermal CO_2 conversion

CO_2 is a very stable molecule and the conversion is not very effective to date. Indeed, the carbon-oxygen bond are relatively strong (783 kJ mol^{-1})[18] and the Gibbs free energy of formation is (ΔG° = -394 kJ mol^{-1})[19], which means that a substantial energy input and optimized condition are required for the chemical conversion to take place.

$$CO_2(g) \longrightarrow CO(g) + \frac{1}{2} O_2(g) \tag{1}$$

The reaction is strongly endothermic, and without removing one of the products (CO or O_2), the equilibrium of this reaction is shifted to the left. Thus, the thermal splitting of pure CO_2 is only favorable and efficient at very high temperatures. As can be seen in Fig

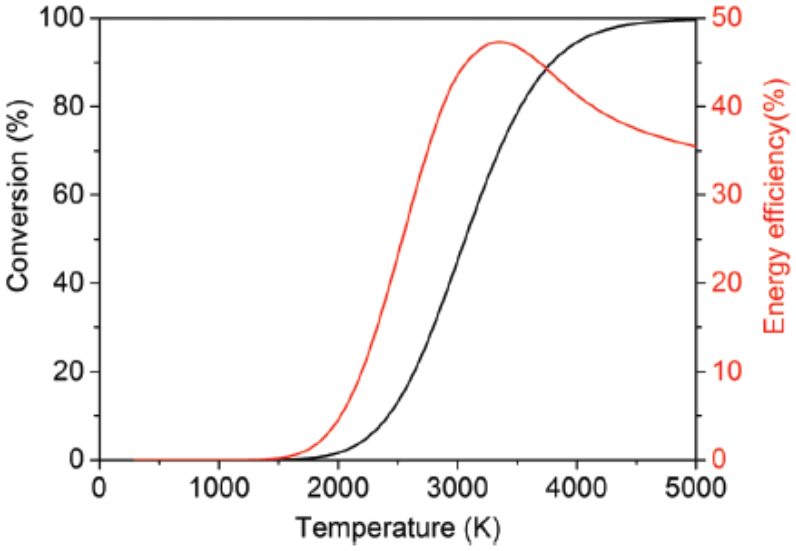

Figure 6: Theoretical thermal conversion and corresponding energy efficiency as a function of temperature for the pure splitting of CO_2 into CO and O_2[2].

6, at 2000 K the reaction is not efficient, hence at 3500 K the conversion overcomes 85% and the energy efficiency is around 47%. On other hand, while the conversion continues to increase with the rising of temperature, the efficiency starts to decrease at 3500 K. In particular, at 5000 K the conversion is 100%, but the efficiency is only 35% [2]. Thus, it

is clear that the pure conversion to CO and O_2 varies from less than 1% below 2000 K and goes up to 85% when temperatures are as high as 3000-3500 K [20].

2.1.2 Mechanism of CO_2 conversion in plasma

The process of carbon dioxide conversion starts, as previously seen, with the splitting of the CO_2.

$$CO_2 \longrightarrow CO + O, \Delta H = 5.5eV \tag{2}$$

Then it continues until it reach a stable situation by oxygen atom recombination into O_2 or an oxygen atom reaction with a co-reactant to create stable molecules [9]. There are many channels enabling CO_2 plasma splitting by ionization: CO_2 splitting by direct electronic ionization impact, CO_2 splitting by vibrational ionization impact, ionization by collision with heavy particles, photo-ionization, surface ionization and CO_2 splitting by pyrolysis at high plasma temperature [21]. The first phenomenon is the CO_2 direct ionization by electronic impact and is achieved by a single impact of neutral or unexcited atoms, radicals, or molecules and CO_2 molecule.

$$e + CO_2 \longrightarrow e + {CO_2}^*({}^1\textstyle\sum {}_u{}^+) \longrightarrow e + CO({}^1\textstyle\sum{}^+) + O\,({}^1S) \tag{3}$$

In the collision, the CO_2 molecule from the ground state, becomes excited with an excitation energy that overcome the dissociation enthalpy in one single step. Then, the molecule de-excites by energy transfer to C==O resulting in a bond breaking. As the lowest electronic level of CO_2 is excited by more than 7 eV, the splitting of the CO_2 molecule by direct electronic excitation is not efficient (Fig.7). The inefficiency is due to the fact that only 5.5eV are theoretically required to break the C==O bond, and thus the extra energy is simply wasted [21]. This typology of splitting mainly happens in a cold plasma or non-thermal discharges, like DBD, where the electron density is high, the average electric field is high, but the excitation level of neutral species remain low. The second process is the splitting of CO_2 by stepwise process by electron impact.

$$e + CO_2 \longrightarrow e + {CO_2}^*(\nu_i) \tag{4}$$

$$e + CO_2 \longrightarrow e + {CO_2}^*(\nu_j) \tag{5}$$

$${CO_2}^*(\nu_i) + {CO_2}^*(\nu_j) \longrightarrow {CO_2}^*({}^3B_2) + CO_2 \tag{6}$$

$${CO_2}^*({}^3B_2) \longrightarrow CO({}^1\textstyle\sum{}^+) + O({}^3P) \tag{7}$$

The CO_2 molecules in the vibrational ground state are first excited to lower vibrational level by electron impact and then the vibrational excited molecules transfer their vibrational energy among themselves in a vibrational-vibrational relaxation process. This

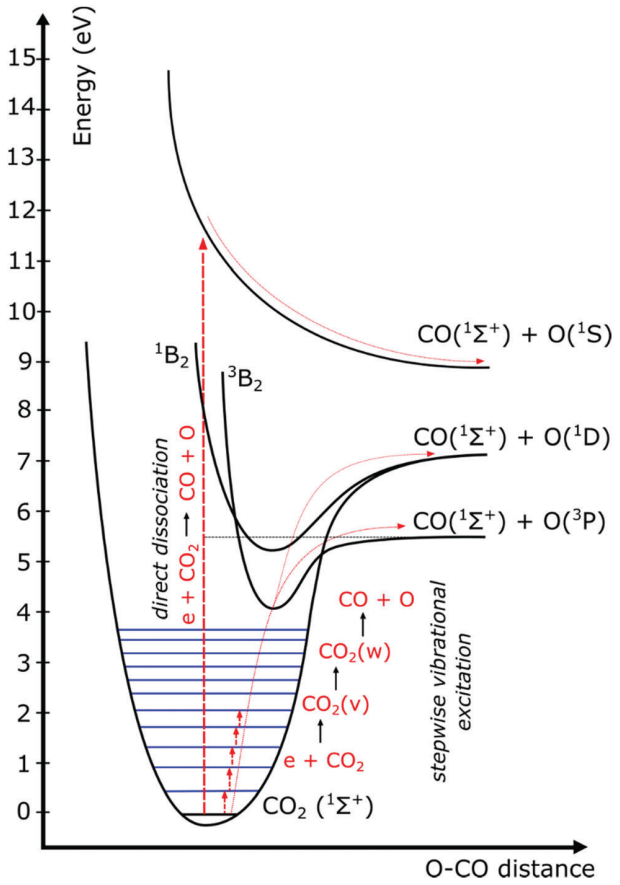

Figure 7: Schematic of some CO_2 electronic and vibrational levels [22]

process is called "ladder-climbing" and requires only the minimum amount of energy for the bond breaking equal to 5.5 eV. Then, there is also a chance that some of them to be pumped up to an higher vibrational energy level at the expense of vibrational de-excitation for other molecules. When the vibrational excitation reaches the dissociation threshold, the CO_2 can split into CO and O in their ground state. This process is quite efficient for CO_2 splitting. However, for the vibrational-vibrational transfer there are two main conditions to be satisfied. The first is the electron temperature of the plasma that has to be at least 1 eV in order to generate enough vibrational dynamics and number of collisions between CO_2 and electrons. The second requirement refers to the transitional temperature of the gas, which must be less than the vibrational temperature to avoid the phenomena of vibrational-translational relaxation. Indeed, this could cause the reduction of CO_2 vibrational level and consequently a lower formation of CO and O molecules. That phenomena is most significant in thermal or energy-dense discharges, where both the ionization degree and the concentration of highly excited neutral species are high [21]. Then the ionization by collisions of heavy particles occurs during ion–molecule or ion–atom interactions, as well as in collisions involving electronically or vibrationally excited species.

In these cases, the total energy of the colliding partners surpasses the ionization potential, leading to ionization. Additionally, the chemical energy of colliding neutral species can also contribute to ionization in processes like associative ionization [21]. Another process could be the photo-ionization that happens when neutral particles collide with photons, resulting in the formation of an electron-ion pair. This mechanism is especially important in thermal plasmas and can also play a role in certain non-thermal discharge propagation processes [21]. Surface ionization occurs when electrons, ions, or photons collide with surfaces, or when surfaces are heated. This process can lead to the release of electrons and is often observed in various plasma interactions with solid materials [21]. The last process is the splitting by pyrolysis at high plasma temperature. As mentioned before, the CO_2 conversion at high temperature increases the degree dissociation up to 85%. Indeed, in the pyrolysis process, the product are CO, O and O_2, with almost no C generated, meaning that the selectivity is close to 100% [9]. The process by pyrolysis has a key problem regarding the reverse reaction that has to be avoided especially when the products leave the high temperature region of the plasma reactor. The three main mechanisms described here for the CO_2 splitting are strictly correlated to the electron density in the plasma. Indeed, in cold plasma and warm plasma, CO_2 splitting is realized by electronic excitation or vibrational excitation, and both are dependent on electron collisions. In thermal plasma, the CO_2 splitting is obtained by electron impact and high temperature pyrolysis. Therefore, the higher the electron density, the more collisions occur, and the higher the conversion rate of CO_2 will be [9]. Fig.8 illustrates the fraction of the energy transferred to the different channels of the excitation, ionization and dissociation of the CO_2 as a function of the reduced electric field (E/n) [22]. The reduced electric field is the ratio of the electric field in the plasma over the neutral gas density and has distinctive values for different plasma types [2].

$$e + CO_2 \longrightarrow e + CO_2(v^*) \longrightarrow CO + O \tag{8}$$

For example, a DBD has a reduced electric field in the range of 200 Td (Townsend) while MW and GA typically operate around 50 Td. From Fig.8 the value of the reduced electric field will have wide application on the distribution of the electron energy among the different channels. Indeed, in the region above 200 Td, most of the electron energy, around 70-80% goes into electronic excitation, about 5% is transferred to dissociation, 5% is used for ionization while 10% goes into vibrational excitation. Around 50 Td the situation is quite different, 10% goes into electronic excitation and 90% of the energy goes into vibrational excitation. Thus, CO_2 dissociation via vibrational excitation (eq. 8) has

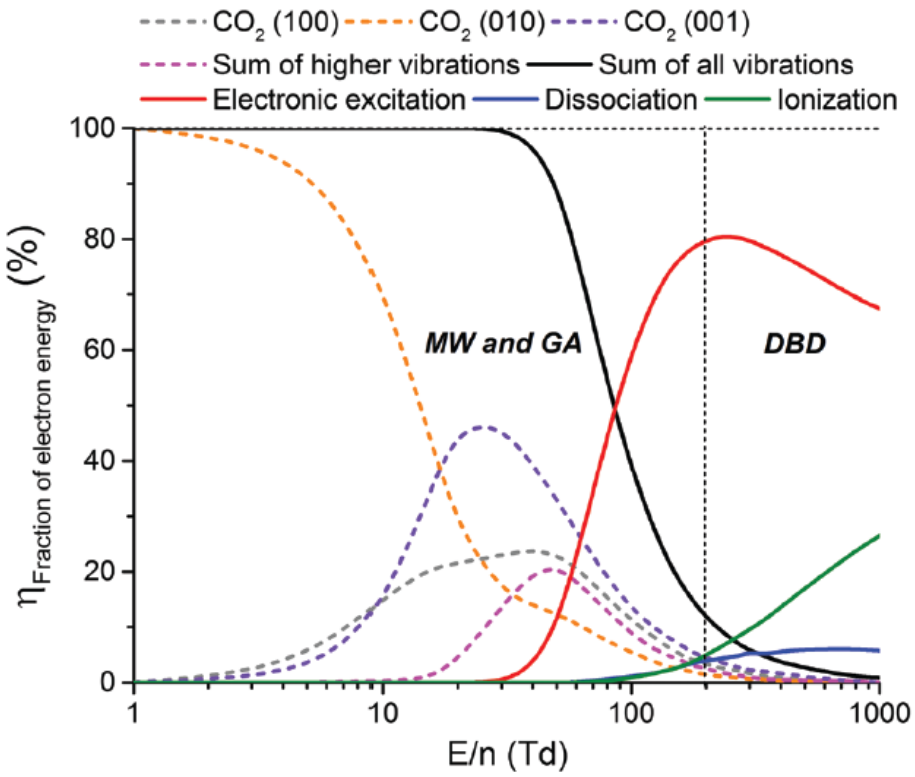

Figure 8: Fraction of electron energy transferred to different channels of excitation as a function of the reduced electric field(E/n)[2]

been considered the most efficient way for CO_2 conversion [11].

2.2 Efficiency metrics

In this section, an overview of the main efficiency parameters including the specific energy input (SEI), conversion (χ), energy efficiency (η) and energy cost (EC) is reported.

2.2.1 Specific energy input(SEI)

The specific energy input is defined as the plasma power imposed by the gas flow rate, which is a dominant factor for the conversion and energy efficiency of a plasma process:

$$\text{SEI (J cm}^{-3}) = \text{SEI (kJ L}^{-1}) = \frac{\text{Power (kW)}}{\text{Flowrate (L min}^{-1})} \times 60 \text{ (s min}^{-1})$$

More generally, the SEI is also expressed in electron volts per molecules, as follows:

$$\text{SEI (eV per molecule)} = \text{SEI (kJ L}^{-1}) \times \frac{6.24 \times 10^{21} \text{ (eV kJ}^{-1}) \times 24.5 \text{ (L mol}^{-1})}{6.022 \times 10^{23} \text{ (molecule mol}^{-1})}$$

2.2.2 Absolute and effective conversion

The absolute conversion is based on the molar flow rates of the reactants, such as CO_2, N_2,Ar or CH_4.

$$\chi_{\text{abs, reactant}_i} = \frac{\dot{n}_{\text{reactant}_i,\text{inlet}} - \dot{n}_{\text{reactant}_i,\text{outlet}}}{\dot{n}_{\text{reactant}_i,\text{inlet}}}$$

Where $\dot{n}$ stands for the molar flow rate of the reactant species i. When more than one gas is present in the mixture, the effective conversion takes the dilution into account:

$$\chi_{\text{eff, reactant}_i} = \chi_{\text{abs, reactant}_i} \times \frac{\dot{n}_{\text{reactant}_i,\text{inlet}}}{\sum_i \dot{n}_{\text{reactant}_i,\text{inlet}}}$$

2.2.3 Energy efficiency and energy cost

The energy efficiency and the cost are related to the process that occurs. In particular, the energy efficiency measures how efficient the process is compared to the standard reaction enthalpy, which is based on the SEI:

$$\eta = \frac{\chi_{\text{Total}} \times \Delta H^{\circ}_{298\,\text{K}}\,(\text{kJ mol}^{-1})}{\text{SEI}\,(\text{kJ mol}^{-1})} = \frac{\chi_{\text{Total}} \times \Delta H^{\circ}_{298\,\text{K}}\,(\text{eV molecule}^{-1})}{\text{SEI}\,(\text{eV molecule}^{-1})}$$

While the energy cost is the amount of energy that is consumed by the process:

$$\text{EC}\,(\text{kJ mol}^{-1}_{\text{conv}}) = \frac{\text{SEI}\,(\text{kJ L}^{-1}) \times 24.5\,(\text{L mol}^{-1})}{\chi_{\text{Total}}}$$

2.3 Dependency parameter

The CO_2 conversion process is affected by different condition such as power supply, pressure, gas flow and co-reactant.

2.3.1 Pressure

The role of pressure in the CO_2 conversion process is crucial, and its impact on energy efficiency and chemical conversion depends on the specific plasma conditions and the technologies used. At high pressure, the density of particles in the plasma increases, favoring a higher likelihood of collisions between particles (electrons, ions, excited molecules) and CO_2 molecules. This increases the reaction rate and can lead to better ionization efficiency. However, if the pressure is too high, the plasma may become too dense, limiting the effectiveness of electron energy generation. In this case, the mobility of electrons is reduced, and the transfer of energy to CO_2 can be less efficient. Furthermore, very high pressure may lead to saturation of reactions, hindering the process. In general, a

moderate high pressure is beneficial for promoting better ionization and control of chemical reactions, but an excess of pressure can cause inefficiencies due to the overly dense plasma [21]. On the other hand, at low pressure, the plasma density is lower, which reduces the chances of effective collisions between electrons and CO_2 molecules. As a result, vibrationally excited species become less energetic, and the ionization process may be less efficient. However, low-pressure plasma allows for better electron mobility, facilitating the creation of excited states and the transfer of energy from high-energy electrons. While this improves the quality of the plasma, the overall conversion efficiency may be lower compared to higher pressure settings, due to the reduced particle density [21]. In summary, moderate pressures tend to offer the best balance between energy efficiency and reaction speed. The conversion efficiency of CO_2 is generally better at higher pressures, as it enhances the ionization and reaction rates, but care must be taken not to exceed a point where plasma density causes energy losses. The process of CO_2 conversion is more efficient at higher pressures, but managing this pressure in combination with other parameters such as frequency and the amount of CO_2 gas fed into the plasma is essential to avoid excessive collisions or reaction saturation. In the microwave plasma technology the energy efficiency can reach up to 90% in supersonic flow conditions at a reduced pressure of 200 mbar [23]. However, so far the value that more is near that target is 51% of energy efficiency, this indicates that technical challenges remain in optimizing the process [24]. Microwave plasma is the most used plasma type in which the effect of pressure is more crucial than all the other types of plasma. To obtain an high value of energy efficiency, the role of the vibrationally excited species is particularly important. Indeed, they need to be energetic enough to generate plasma which consist of high electron temperature, high specific energy input and ionization degree [21]. To obtain that effect the microwave can operate in two ways, diffusive regime and contracted regime, depending on the operating temperature(Fig.9). At low pressure (25-65 mbar) the operating condition of microwave discharge is in the diffuse regime, while increasing the pressure it become contracted regime. This phenomena is important because by regulating the operating pressure, the energy transferred from the electrons to the working gas change. [24] demonstrate that increasing the pressure leads to a drop of both the CO_2 conversion and the efficiency since the energy loss during the collisions between electrons increases. However, atmospheric pressure is still preferable for the CO_2 conversion compare to new experiment at low pressure condition using a vacuum pump. Hence, while stable molecule like CO_2 are under investigation microwave atmospheric pressure discharge is preferred than vacuum conditions [25].

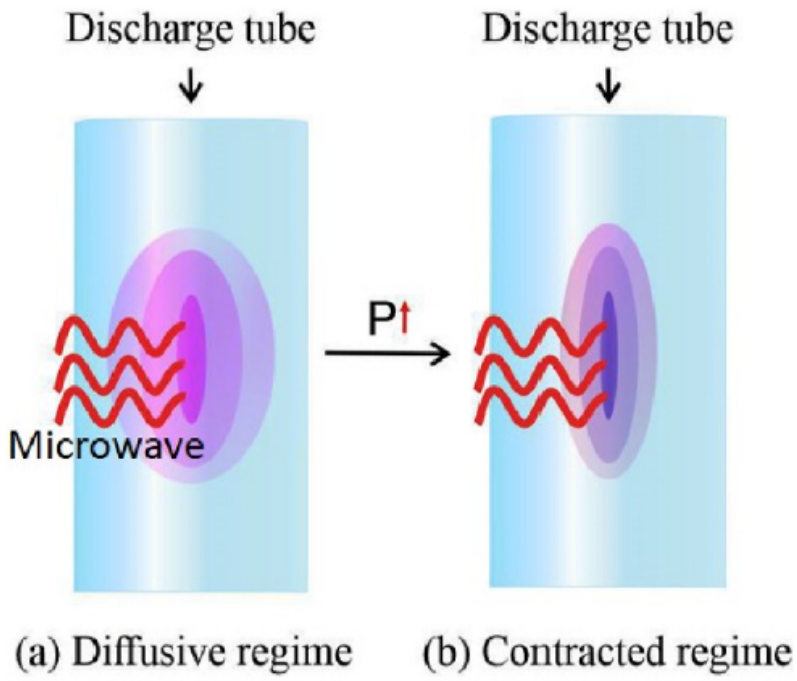

Figure 9: The transition of a microwave discharge from (a) diffusive regime to (b) contracted regime as the pressure increase [25]

2.3.2 Power supply

Another parameter that can change the energy efficiency is the power supply. This is because different power will results in different power density and so different electrons molecules collisions frequencies[26]. Power density is defined as the absorbed microwave power per unit volume and is directly proportional to the density of electrons. As mentioned previously, electrons are accountable for the very first step of CO_2 dissociation as the lighter electrons absorb most of the applied energy and activate the inert gas molecules through collision. The energy transferred is highly dependent on the power supply. The higher the power is, the higher the average electron energy, so the plasma region will be extended and eventually increase the retention time of the reactants within the plasma region. Also the power interruption has be found to have a positive effect on the decomposition of the CO_2, this because it can modify the electron energy distribution. Finally a CO_2 conversion process can be enhanced by synchronizing the plasma pulse duration with the residence time of the gas[27]. A clear example can be given by fig.10 where a DBD reactor performs an analysis with different input power with the parameter discharge frequency equal to 9 kHz and feed flow rate equal to 50 mL/min. The increasing of the input power leads to an higher conversion reaching a maximum of 8.15% when the

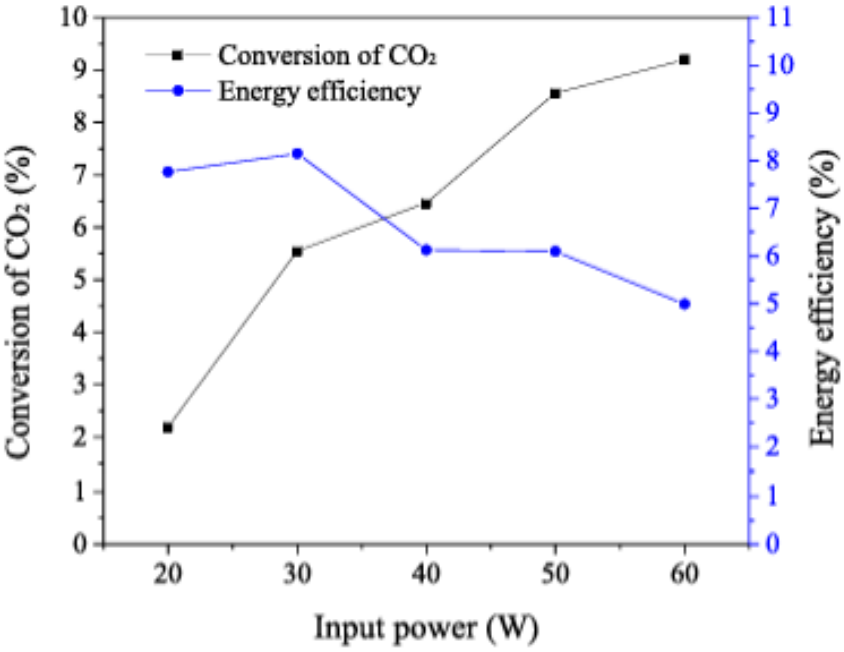

Figure 10: Effect of input power on CO_2 conversion and energy efficiency[28]

input power is equal to 30 W and decreases to 4.99% at 60 W, while the energy efficiency goes into the opposite way[28].

2.3.3 Gas flow and co-reactance

The efficiency is then also strictly correlated to the gas flow rate and the way in which the gas is fed. By adjusting the gas flow rate, the residence time of the reactant in the plasma region changes, which in turn affects the frequency of electron collisions with the excited species. When the gas flow rate is modified, it determines how long the reactants stay in the plasma, and this time of residence influences how often electrons interact with the species present in the plasma. If the residence time is too short, the electrons may not have enough opportunities to collide with the excited species, reducing the efficiency of the process. Conversely, if the residence time is too long, the reaction might not be optimal, and the efficiency could decrease due to excessive relaxation of the excited species or other competing processes. Therefore, finding the right balance in the gas flow rate is crucial to optimize the frequency of collisions and maximize the efficiency of the plasma process. Indeed, the way of which the gas is supplied could be: downstream, upstream and up-stream vortex [24]. The downstream configuration give the lowest value of conversion and energy efficiency due to the low quenching of the exhaust gas and thus allow the recombination of CO into CO_2. On the contrary, the vortex gas configuration resulted

in the higher energy efficiency. This because the gas pattern enhance the quenching effect of the gas during the cooling stage. As a result of that the resident time of the reactance increase as well as the plasma stability giving a better conversion of the CO_2. Furthermore, the upstream vortex has resulted to be better than the downstream one, this due to the excited species that are kept together in the plasma volume[27]. By adjusting the gas flow rate, the reactant residence time changes in the plasma region and thus affect the collision frequency of the electrons with the excited species. A clearly example is given by fig.11 in which until a certain limit the conversion continuing increasing, then it drops and the efficiency starts to rise due to the decrease of the conversion [29]. Another illustration can be given by fig.12 in which as same before, the conversion rise until a value which make the residence time higher and a lower production of CO is recorded[28]. This phenomenon can be explained in that way, by decreasing the CO_2 rate the residence time of the reactants extends, this admit the reaction system which gives opportunities for them to collide with energetic electrons and excited species, and then results in an improvement of conversion process. On the contrary, with the higher CO_2 flow rate, the concentration of CO species decreases, but the amount of CO_2 molecules that can be dissociated increases on the whole. That results in an increasing of the energy efficiency due to an availability of input energy.

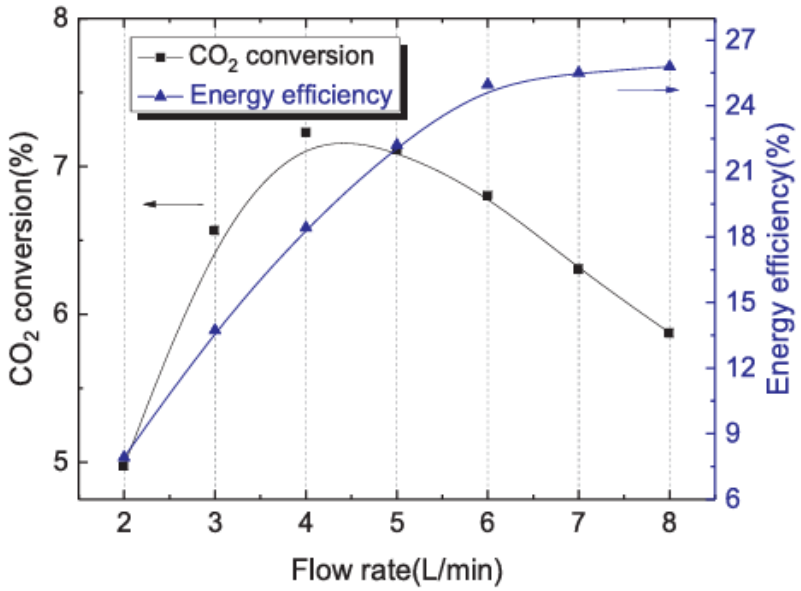

Figure 11: Effect of gas flow rate on the CO_2 conversion and efficiency[29].

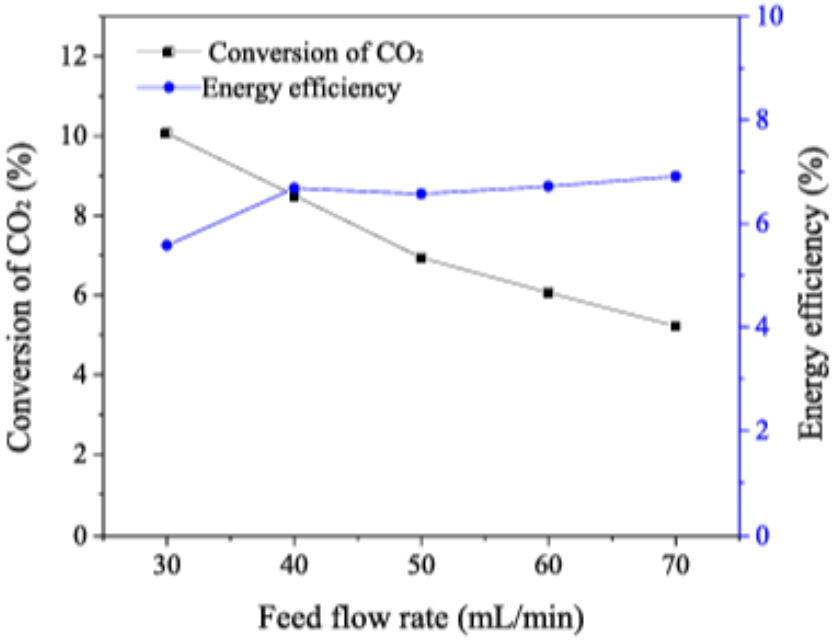

Figure 12: Effect of feed flow rate on CO_2 conversion and energy efficiency[28].

Beside that,The role of the carrier gas in improving the efficiency of CO_2 conversion to CO is closely tied to its ability to influence the properties of the plasma and the dynamics of the chemical reactions. Carrier gases such as argon (Ar), nitrogen (N_2), and helium (He) are the most commonly used [30] and contribute to enhancing the electron density in the plasma, which is essential for the excitation and ionization of CO_2. Ar is useful for maintaining plasma stability, promoting the production of high-energy electrons that interact with CO_2, without generating too many undesirable by-products, as happens with N_2 [31]. Another important aspect is the gas temperature. In non-thermal plasmas, heavy particles such as carrier gas atoms remain relatively cold, while high-energy electrons are hot enough to excite CO_2. This allows the energy from the electrons to be transferred primarily to CO_2 without excessively heating the gas, which makes the process more efficient. Carrier gases help maintain a balance between energy and temperature, promoting more efficient conversion [32]. Finally, carrier gases can also improve the kinetics of CO_2 reduction reactions, increasing the likelihood that the desired reactions will occur. An optimized carrier gas flow can extend the residence time of reactive species in the plasma, promoting CO_2 dissociation and increasing CO production. Finally, the presence of carrier gases such as argon and helium can stimulate the formation of excited species, like CO* and O*, which are particularly effective in facilitating CO_2 splitting and improving reaction yield [33]. This effect is due to the additional reaction route for CO_2 dissociation that occurs when an inert gasses is mixed in the fed gas. The results will be reported as

an increase of the CO and O atomic lines detected by the OES.

$$N_2^* \text{ (or } Ar^*) + CO_2 \rightarrow CO + O + N_2 \text{ (or Ar)}$$

Despite the positive effect, N_2 could easily increase the conversion of the CO_2 but the decomposition of N_2 will result in unwanted product like NO_2,NO and N_2O. Its presence in the plasma can increase the energy transferred to the particles, aiding the dissociation of CO_2 into CO and O. However, the use of nitrogen must be carefully controlled to prevent the formation of these harmful compounds. Although, the presence of that molecules and the elimination of partial O species has a huge positive effect to limit the reverse reaction. Thus enhance significantly the CO_2 conversion.

$$O + CO + M \rightarrow CO_2 + M$$

Helium enhance the process of CO_2 conversion but it is much more expensive than Argon and has an higher ionization potential which leads to a lower results than He[33]. Finally the most valuable result are obtained by adding N_2 in the flow rate than the other inert gasses due to a stronger CO_2 promotion. A simple comparative result from Ar/CO_2 and He/CO_2 can be seen in fig.13 in which the fraction of CO_2 continuous increase in the range 5%-95%. The value of conversion is lowest when the amount of CO_2 is higher. Until the 70% of CO_2, the trend is similar and there are almost no differences between Ar and He, but below this value the boost of the Ar become predominant reaching a value of 41%[32].

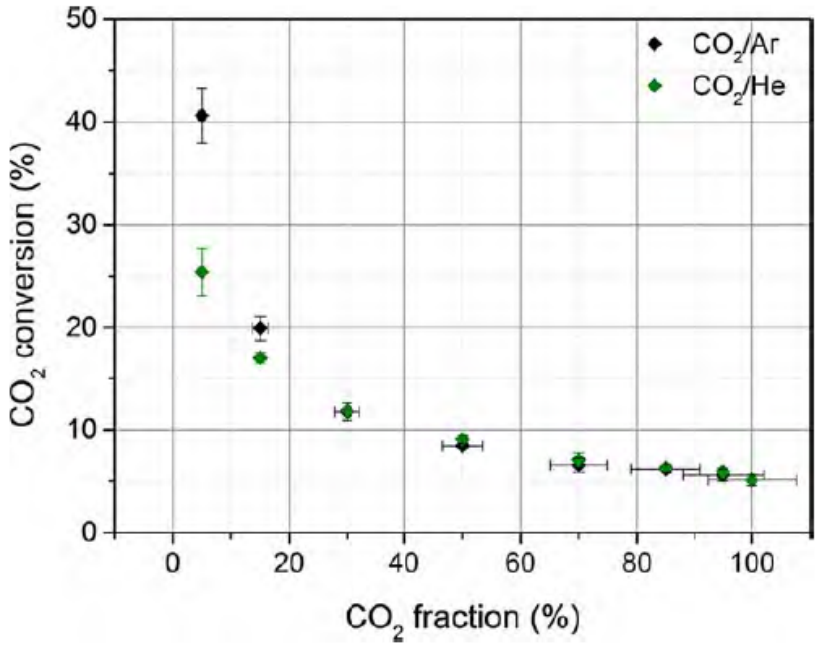

Figure 13: CO_2 conversion as a function of CO_2 fraction in CO_2/Ar and CO_2/He gas mixtures[32].

2.4 Comparison of splitting CO_2 with different plasma

In this section the comparison between the existing plasma based technology for CO_2 with DBD, MW and GA plasmas conversion are investigated. In particular with the main focus on improving the energy efficiency of the conversion and the selectivity toward value added chemicals. As outlined before, in case of pure CO_2 splitting, the main product are CO and O_2. So, the reaction is a simple chemical process and the wide variety of product that can be formed are not investigated in this section. Only the focus on the optimizing the CO_2 conversion and the energy efficiency[2].

2.4.1 DBD plasmas

The most common geometry used for DBD plasma to study the CO_2 splitting are coaxial DBD reactor[34] and parallel plate reactor[35]. To achieve higher value of CO_2 conversion and energy efficiency, several approaches have already been investigated, including changing the applied frequency, gas flow rate, discharge gap, applied power, dielectric material, electrode material, mixing with gases and catalysis.

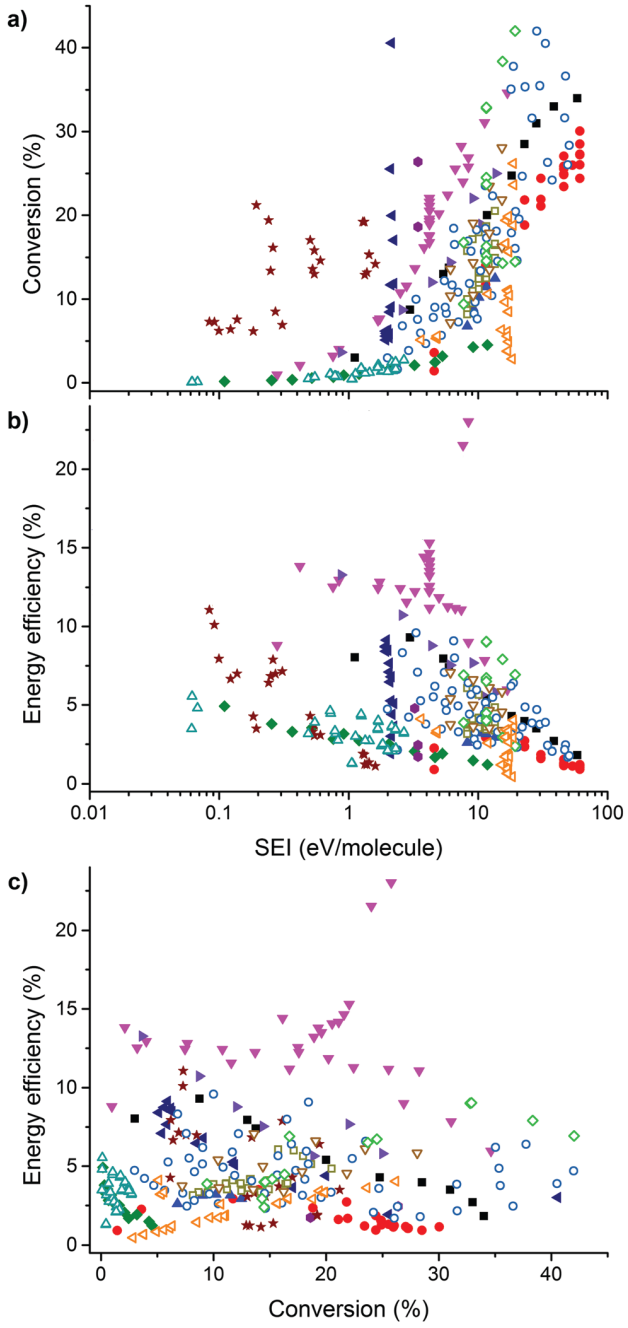

Figure 14: Experimental data collected from the literature for the CO_2 splitting in a DBD, where *a)* and *b)* show the conversion and energy efficiency as a function of SEI, while *c)* depict the energy efficiency as a function of the conversion. All the data represent experiment that has been done with many different configuration, in particular the open symbol represent data with catalysis[2].

From Fig 14 the main trend are pretty evident, the conversion increases with the increasing of the specific energy input, while the energy efficiency generally decrease with the increasing of the SEI, especially above 10 eV per molecule. In the plotting of energy efficiency as a function of the conversion, almost all the result are below the 15% and 40%

for the conversion. The highest value of conversion is obtained with a packed bed DBD and reach about 42%, while the highest energy efficiency was 23%, obtained by a pulsed power DBD. One of the most crucial parameter for the conversion of CO_2 is the SEI, but as can been observed, with the same value of SEI the conversion reach different result. So, an another key parameter is the gas flow rate, and consequently the residence time, which has an extremely important effect on the balance of the conversion. Furthermore another important aspect is that a lower power, with a lower gas flow rate will result into an higher conversion efficiency than an higher power with an higher gas flow rate at the same SEI[36]. Other changing that have been made are regarding the geometry, specifically the discharge length and discharge gap. In particular varying the discharge length, at the same SEI, has no significant variation on the discharge characteristic, conversion and energy efficiency[37]. On other hand, the discharge gap seems to change the discharge behaviour and so the conversion of the CO_2. Studies have demonstrated that above a gap width of 3.3 mm less streamer formation occurs, leading in a less efficient plasma volume, hence lower conversion and efficient results[36]. Also the applied frequency seems to have a negligible effect on the conversion and energy efficiency. Even if the plasma seems to be more filamentary at high frequency (75 kHz) compare to low frequency(6 kHz)[38]. Then also the gas temperature is an important parameter that govern the reaction rate. For the plasma based conversion with DBD the effect is not so clear, because a linear increase of the conversion is obtained from 303 K and 443 K, but discrepancy of the results are reported[34][38]. The effect of the dielectric material in the DBD is another topic very debated by studying the formation of a selective coating. Indeed, the conductivity of the dielectric material can play an important role for the discharging proprieties. Several test has been made using alumina and quartz with the results of a better reactor stability and reaching an higher conversion[38]. In the meanwhile other material are under investigation with the addition of calcium and boron[39]. However, from the calculation of the plasma power, it appears that more sophisticated dielectric mainly increase the efficiency of the plasma power, and not the effective plasma conversion efficiency. In any cases these dielectric allow operation at less voltage which could be beneficial in certain process[2]. Also the electrode material has been investigated, Cu and Al increase the conversion with a factor 1.5 compare to Fe electrode. Furthermore Al electrode has shown a maximum energy efficiency three times higher than Rh electrode under the same condition. But, on other hand the problem of chemical corrosion and sputtering are not negligible and represent a huge problem for this type of material[40]. As mentioned above, also the adding of inert gases, such as N_2, Ar and He, could ignite

the plasma more easily. This also affect the discharge characteristics, energy efficiency, conversion and by-product formation. The addition inert gasses such as He and Ar, leads to an increase in the CO_2 conversion, but the effective conversion decreases, since there is less CO_2 present in the mixture and the increased conversion is not sufficient to counteract this drop in the CO_2 fraction[40]. On other hand, the presence of N_2 strongly increase the effective conversion and energy efficiency up to 50%. However, unwanted product like N_2O and $NO_x$are produced using N_2[41]. Finally the backed bed reactor in a DBD has been investigated with great result for the energy efficiency and conversion. Different materials have already been investigated such silica gel[42], Al_2O_3[43], ZrO_2[44], SiO_2[43], $BaTiO_3$[45], MgO[46] and CaO[46]. The best results have been obtained with ZrO_2, CaO and CeO_2[47], with conversion in the range of 30-45% and energy efficiency in the range of 5-10% (Fig.14(c)). One of the most recent studies refers to a protocol for the dimension of the particle size in the packed bed reactor. More specifically, with a size of particle around 180-330 μm, the conversion increase up to 70%. However, also the breakdown voltage increase, leading to a partial discharging so a drop in the fraction of the reactor where plasma formation occurs[45]. From all the recent studies DBD reactor can reach a conversion up to 40%, but the energy efficiency is far away from the target equal to 60%. As a matter of fact DBD have the advantage to be scalable and is very easy to operate.

2.4.2 MW and RF plasmas

The dissociation of CO_2 with MW and RF plasmas have already been used some decades ago[21], but gained more interest in the recent global challenges regarding the CO_2. Already in the last century, it was concluded that MW plasma was ideal to obtain high energy efficiency for the CO_2 conversion due to a relatively high electron density and a low reduced electric field. These condition are particularly favorable for the excitation of asymmetric mode vibrational levels of CO_2[48]. This efficient dissociation is a combination of several reaction steps: the excitation of the lower vibrational levels by electron, followed by collision between vibrational levels that gradually populates the higher levels, and dissociation of the excited vibrational levels stimulated by collision with other molecules[49]. As for the DBD, also for the MW and RF plasmas different configuration are already been discussed. In particular to obtain the best value for energy efficiency and conversion, these factor have been changed: gas flow rate, applied power, reactor geometry, flow typology, gas temperature and by introducing catalytic materials.

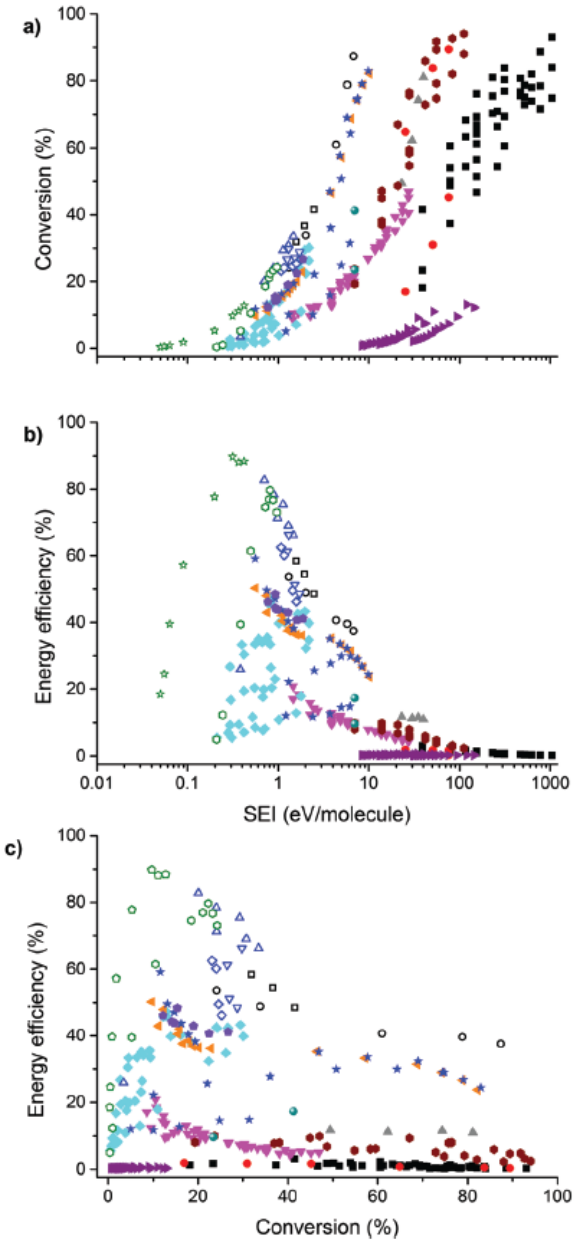

Figure 15: Experimental data collected from the literature for the CO_2 splitting with MW and RF plasma, where *a)* and *b)* show the conversion and energy efficiency as a function of SEI, while *c)* depict the energy efficiency as a function of the conversion. All the data represent experiment that has been done with many different configuration, in particular the open symbol represent data with catalysis[2]

From Fig 15 the highest value of energy efficiency are 80% in subsonic flow conditions and 90% for supersonic flow and performed at reduced pressures[48]. Recently the value of efficiency reached are 50% with both the plasmas[50]. The result obtained, especially, were near the thermal dissociation limit indicating that the thermal dissociation limit are predominant in this typology of plasmas. As for the DBD, the conversion increases with

the increasing of the SEI, while the energy efficiency decreases above an SE of 0.1-1 eV per molecule. While, as regard the energy efficiency as a function of the conversion, all the studies results typically an energy efficiency of 10-50% in the entire range of conversion of 95%. For the MW discharge the same trade off between energy efficiency and conversion as a function of SEI is present[50]. To successfully increase the energy efficiency, it is needed to be able to increase the conversion degree without increasing the specific energy input of the system, which essentially requires using techniques other than increasing the input power[51]. As already mentioned, the pressure has one of the most important role in the MW plasmas and on the CO_2 conversion. The main reason is that at low pressure the recombination reaction becomes negligible[52]. An optimum operational pressure has to be around 150 mbar, but all depends on the operational conditions, such as gas flow rate[50]. Several types of flow and geometry have been already tested to optimize the MW discharge performance for CO_2 conversion. Supersonic flows have been proven to reduce the losses of vibrational levels upon collision with ground state molecule and allowed to achieve energy efficiency up to 90%[50]. Like DBD, the addition of other gasses to CO_2, such as Ar[53], He[54] and N_2[33], could have a critical role for the CO_2 conversion. The presence of Ar results in no effect on CO production, leading to not affecting the collisions processes benefiting dissociation[53]. On other hand the overall CO_2 conversion reach higher value when diluted with Ar instead of He, furthermore the conversion increased but the energy efficiency decreased when adding more Ar or He[54]. The presence of N_2 instead, could play an important role in a different way with the respect of DBD plasmas. Indeed, in the MW plasma the improvement of the CO_2 conversion is by vibrational excited N_2 molecules[33], while for DBD is by meta-stable electronically excited N_2 molecules[41]. The energy difference between the first vibrational level of N_2 and CO_2 is very small, making the fast resonance transfer of vibrational energy from N_2 to CO_2 possible. As such, N_2 can help with the vibrational pumping of CO_2 and thus can enhance the CO_2 conversion. On the other hand, the vibrationally excited N_2 molecules can also react with O atoms, leading to the production of NO_x as was also observed for a DBD[33]. Finally the role of the catalyst has already been tested, in particular in the post discharge configuration using Rh/TiO_2[53] and NiO[55]. The result obtained figured out how the implementation of a packed reactor could increase the efficiency by a 17% in a post discharge zone configuration. However, this increase was suggested to arise from the dissociation of CO_2 at the catalyst surface with oxygen vacancies through dissociative electron attachment, which is a less efficient dissociation process than the step-wise vibrational excitation. The role of the catalyst in the future could be to reduce the

E/n value of discharge due to physical effect or stimulating the dissociation of vibrational excited CO_2 molecules on the surface[2]. Overall MW technology are capable to overcome the 60% efficiency mark for CO_2 splitting and reach an energy efficiency of 45-50%.

2.4.3 GA plasmas

The GA set up tries to combine both the advantages of the DBD and the MW, offering to work at atmospheric pressure and reaching the most efficient dissociation process through vibrational excitation[56]. The two main configuration used are a simple 2D electrodes blade and a the GAP (gliding arc plasmatron) configuration that is based by a cylindrical electrode. The former, has the disadvantages to have a residence time in the plasma quite low, the flow rate is limited and only a limited amount of gas i processed to discharge[57], leading to a maximum conversion of 20%[58]. The latter, ensure a longer residence time in the discharge zone at higher flow rate, reaching a 40% of gas flow that can be processed by discharge[57]. Beside those geometry variations, other works focused on changing different parameters like applied power,flow type, interectrode gap, admixture gases, gas flow and plasma chemistry. From fig.16 the highest energy efficiency obtained is around 40-50%[59] while the highest reported and calculated is equal to 65%[58]. In general the main trend of energy efficiency and conversion as function of SEI is equal to the ones of DBD and MW. The conversion increases and the energy efficiency decreases with the increasing of the SEI, and the optimal range of SEI is 0.1-1 eV per molecules. For a regular GA, the conversion increases and the energy efficiency decreases when more power is supplied[58]. The GAP can operate in two regime that depends on the power input (low and high current regime) with the highest energy efficiency, the lowest conversion observed for the former and the opposite for the latter[59]. Then, lower the gas flow rate is and higher will be the conversion due to a longer residence time of the gas in the discharge[59].

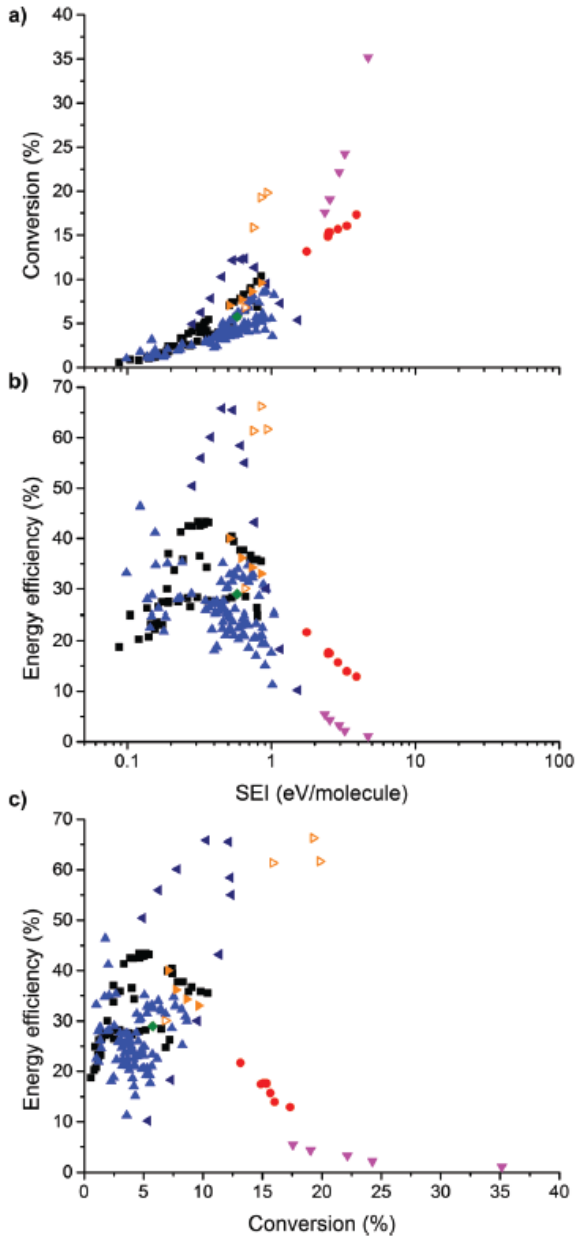

Figure 16: Experimental data collected from the literature for the CO_2 splitting with GA plasma, where *a)* and *b)* show the conversion and energy efficiency as a function of SEI, while *c)* depict the energy efficiency as a function of the conversion. All the data represent experiment that has been done with many different configuration, in particular the open symbol represent data with catalysis[2]

Another important parameter is the vortex flow type, which can be modulated by adjusting the reactor geometry[56]. Operating in a reversed vortex flow (RVF), compared to a forward vortex flow (FVF), it provides an increase in residence time. As a result, the RVF delivers higher energy efficiencies at higher SEI values, leading to an improved conversion[59]. It is also this vortex flow that allows for the higher gas flow rates to be

processed compared to a regular GA, and theoretically also to obtain higher maximum conversions because the gas passes through the arc in the longitudinal direction, thereby yielding a longer residence time. For the GA, also the interelectrode gap can vary to improve the CO_2 conversion, and the best result was observed for the smallest interelectrode distance. Indeed, increasing this distance leads to a larger arc volume and a corresponding drop in plasma power and electron density, and consequently also a drop in CO_2 conversion[58]. Furthermore the addition of N_2 leads to a positive effect for the conversion, but unwanted product like NO_x are also produced[60]. In summary, the GA is the most efficient CO_2 dissociation channel based on vibrational excitation while operating at atmospheric pressure. Energy efficiencies of 45% and even results above the target value of 60% have already been reported. Further exploitation can be done by model calculations on the non-equilibrium character of the GA to increase the energy efficiency[60].

2.4.4 Summary of the type of plasma

To sum up, in Fig.17 are plot the energy efficiency as a function CO_2 conversion for all the types of plasma with the thermal equilibrium and the target of energy efficiency. From Fig.17 it is clear that, DBD are the most extensively studied typology for CO_2 but

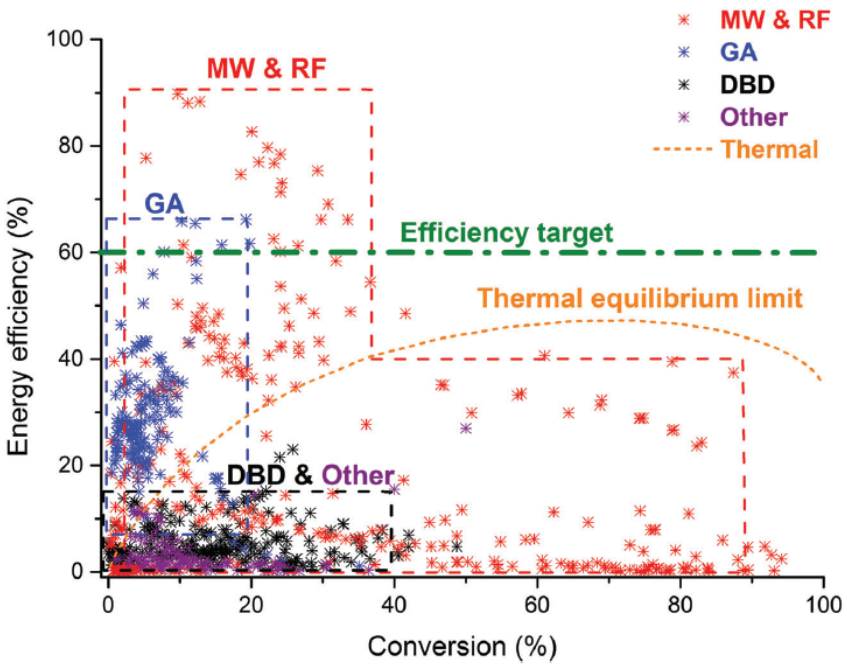

Figure 17: Comparison of the data collected from the literature for CO_2 splitting in the different plasma types, showing the energy efficiency as a function of the conversion[2]

they seems to be unsuitable for an efficient conversion. The value of the efficiency remains

a factor four time too low in order to try to compete in the industrial scale. The GA plasmas results to reach the set energy efficiency target of 60% and almost all the result are above the thermal equilibrium limit, which is very interesting especially due to the operation at atmospheric pressure. This demonstrate that the non-equilibrium character of this type of plasmas are able to exploit the energy efficient dissociation of the CO_2 vibrational levels. Furthermore, advanced modelling of this system could even enhance the energy efficiency. On other hand, the main challenge of thus technology is the limited conversion that remains below 20% due to the limited part of the gas that goes thought the plasma. Finally the MW plasmas can be used for a wide variety of possibilities. At the value of conversion equal to 40%, the energy efficiency target is easily crossed and it could operate in the non-equilibrium regime, which is favorable for the step wise vibrational dissociation mechanism. Conversions in the range of 40–90% are also possible, but the efficiencies reaches up to 40% and the working condition are in the thermal regime[2].

2.5 Synergistic effects of plasma catalysts on CO_2 conversion

The synergistic effect of plasma catalyst has a great potential and is able to enhance the CO_2 conversion, the target product, the selectivity and the energy efficiency due to the physical and chemical interactions.[61]. The plasma catalysis synergy has a major advantages with the respect of combining separately non-thermal plasma with a catalyst. So, the net effect of plasma-catalyst on the reaction is greater than the sum of the individual effects that the catalyst and plasma have on the reaction when used independently[62]. When investigating the synergistic effects of plasma-catalysis, it is important to understand the chemical and physical effects of combining catalysts with the plasma[11]. CO_2 conversion can be increased by chemical effect as a result of the interaction between CO_2 and the catalyst. In particular, the catalyst can also modify the selectivity of the reaction and so the target products. In the meanwhile, the physical effect can increase the efficiency of the process, this by rising the local electric field, which produce more reactive species and increasing the electron density of the plasma; leading to a more CO_2 converted without increase the discharge power[11]. However, both chemical and physical effects are often connected each other and cannot always be distinguished due to the complex interactions occurring between the plasma and the catalyst[61]. This reactions can be summarized in two main categories:

1. The effect of plasma on the catalyst
2. The effect of catalyst on the plasma

The most common plasma effect on the catalyst are:

- surface structure and morphological changes in the catalyst resulting in improved dispersion and a larger active surface area[63];
- change of reaction pathways or creation of new reaction routes due to the availability of a wide range of reactive species, including excited species;
- lower activation barriers and higher pre-exponential factors as a result of the formation of vibrationally excited species;
- formation of catalyst surface hot spots due to small micro-discharges;
- collision induced surface chemistry.
- chemical and electronic changes on the catalyst surface that may change the catalyst oxidation state, leading to a change in the catalyst work-function, thus could be associated to the current voltage that alter the work function of the catalyst[64].

Then the ones related to the effect of the catalyst on the plasma are:

- an enhancement of the electric field through the geometric distortion and surface roughness;
- the formation of micro-discharges inside the pores of the catalyst material, due to the very strong electric field inside the pores, leading to different characteristics compared to the bulk;
- a change in the discharge type, because the presence of insulating surfaces promotes the development of surface discharges;
- the adsorption of species on the catalyst surface, which affects their concentration and conversion due to longer retention times.

The most common catalyst effect on the plasma are the increasing of the electric field near the surface of the catalyst using a DBD[65]. This is typically influenced by the amount of catalyst used to pack the discharge zone of the reactor, which can alter the discharge mode of the plasma. Changes in discharge mode are mostly the result of a reduction in the void fraction of the discharge zone with packing. Other could be the partial package of the discharge zone that maintains a large void fraction and typically produces strong filamentary micro discharges without causing much of a change in the

discharge mode[66]. Furthermore, packing generally produces more effective polarization at contact points between the catalyst pellets and between the pellets and the reactor walls which strengthens the electric field[67]. This produces a stronger discharge than an unpacked reactor and has a strong effect on the electron energy and density in the discharge zone. At a given potential, a fully packed discharge zone shows more effective polarization than a partially packed one due to the increased number of contact points, resulting in enhancement of the electric field and producing electrons with a higher average electron temperature[66]. These electrons can activate molecules in the plasma and generate species that can undergo reactions on the catalyst surface. However, the average electron density and reactant residence time in a fully packed DBD are lower than a partially packed or unpacked configuration, which can hinder the reactor performance[43].

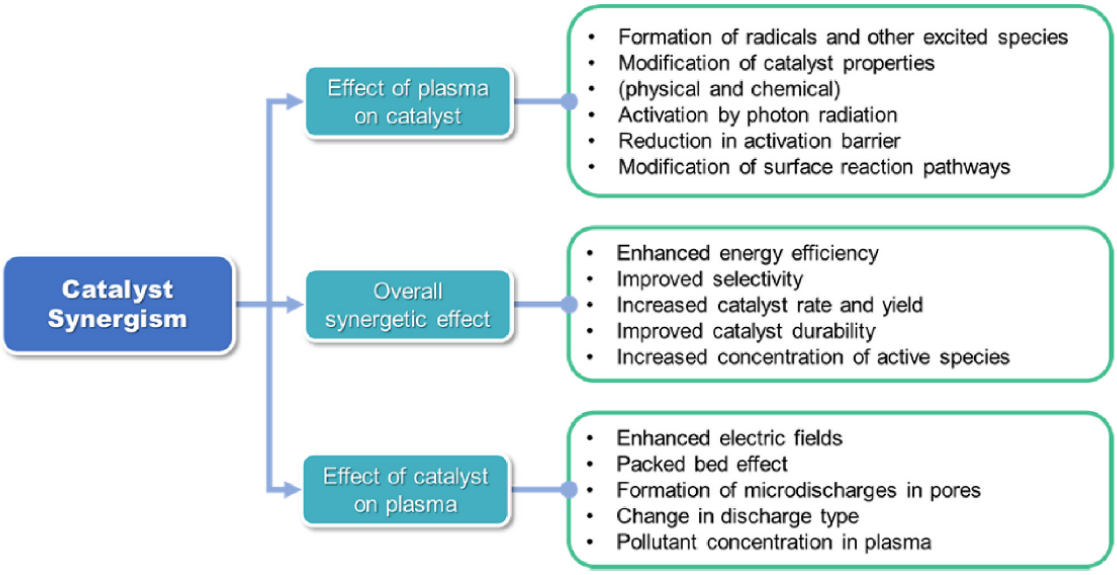

Figure 18: Overview of possible effect of the catalyst on the plasma and vice versa[11]

.

2.5.1 Principal catalytic material

Among all the different types of plasma, the DBD is the most investigated one regarding the catalytic material. Indeed, in comparison to all the other types of plasma several solution have already been proposed with value of conversion very promising. Previous studies have demonstrated that introducing oxygen vacancies improve the reaction performance and help to understand the relationship between the active surface and plasma[68]. One of that is surely the CeO_2 which result in a ability to alter the oxygen

concentration without changing the phase, in particular it provides a large and stable oxygen storage capacity and it is used for many catalytic application[47]. Furthermore CeO_2 provide also an active site for adsorption and activation of molecule that contains oxygen[69]. On other hand, also the ZrO_2 pellets seems to have a positive effect. Thus can be explained especially for the more stable, uniform and stronger discharge because it meant that more CO_2 molecules where activated[70]. In this section three main configuration using CeO_2[68], ZrO_2[70] and the mixing of both[47] are investigated by changing the most important parameter. Starting with the CeO_2 catalyst in a DBD reactor with different morphologies (cubes, rods and hexagons)[68]. All the experiment with this configuration has been made in atmospheric pressure, frequency ranged from 8.9 to 9.1 kHz, the catalysts fully packed in the discharge region to keep packing volume the same and finally the catalyst has been granulated and sieved into a 40-60 mesh size[68]. The main investigation that have been made using the CeO_2 catalyst are obtained by varying the discharge voltage and input power. As can be illustrated from fig.19(a) with an increase of the discharge voltage, the CO_2 conversion of all the catalysts increase, with the highest conversion reached by the rods catalyst configuration. When the discharge voltage reach the 11 kV, the difference in the performance become smaller and the conversion reach around 20-25%. In Fig.19(b) the catalyst has been evaluated with the same input power, the difference between all the catalyst become smaller when the input power overcome the 10 W, this indicate that the effect of the catalyst at high input power become less relevant. This behavior can be attributed by the lower energy efficiency that the rods catalyst reach while it operate at different discharge voltage (Fig19(c)). Indeed, at the same input of power the rods catalyst show a lower discharge voltage and less CO_2 conversion. On other hand, as shown in Fig.19(d) it present the higher power efficiency with the respect to all the other type of catalyst[68]. Another commercial catalytic material are the ZrO_2 pellets combined together with the glass beads and used ad packed materials. In that case several factor, such as discharge power, discharge length and bead size, are taking into account to investigate the CO_2 conversion[70]. The main parameter considered were: frequency equal to 12 kHz, flow rate equal to 20 mL/min. To better understand the influence of the discharge length into the unpacked DBD reactor an analysis has been made and can be seen in fig.20[70]. In particular, it can be seen that the decomposition rate increase with the increasing of the discharge length. This is due to the higher residence time of the CO_2 inside the reactor, which enhance the probability of molecules to collide each other with an higher energetic electrons and reactive species[71]. Despite that, a longer discharge region will require also an higher surface area of the BDB reactor, which means

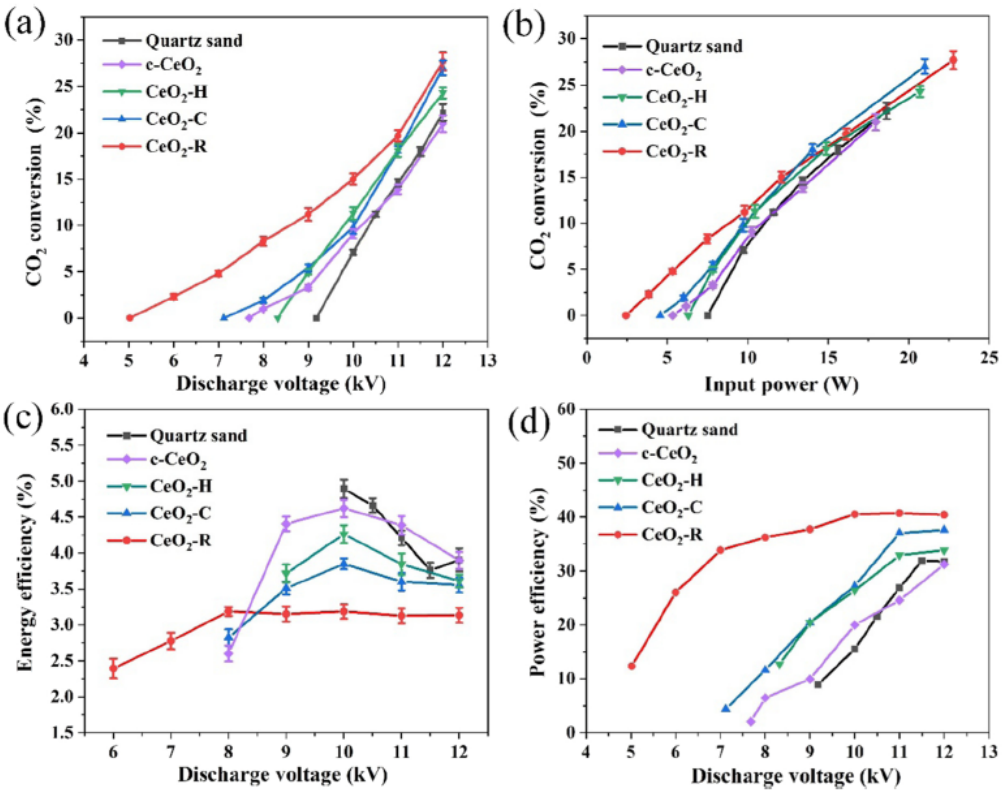

Figure 19: CO_2 conversion, energy efficiency and power efficiency as a function of applied voltage and in input power of CeO_2 catalysis[68]

also higher energy losses and dissipation(fig.20(b))[72]. In the case of ZrO_2, increasing the discharge length have more dominant effect with the respect to the negative effect. A second analysis is reported in which can be seen the effect of the CO_2 decomposition as a function of the discharge power and on the bed size. In fig.21 can be seen that smaller is the bed size and more beneficial effect are obtained. In particular, when the beds size decreased, more dielectric sphere would be needed, which increased the surface area and reinforced the surface discharge, hence an higher CO_2 decomposition rate is reached[44]. Discharge is also a key factor, indeed the discharge power determine whether there was sufficient energy for activating and decomposing the CO_2[73]. The influence is reported in fig.21(a)(b), where the degradation rate increase with the increasing of the discharge power, but the energy efficiency decrease. An higher discharge power meant more energy into the system, therefore generating more active species and reactant molecules in the reaction, and enough energy would activate electron and reactant molecules, as well as increase the mutual collision opportunities between active species, so more chemical bonds would be broken and more active substances formed[70]. However, the decomposition of the CO_2 tends to saturated above the 55 W, thus means that a suitable range of discharge

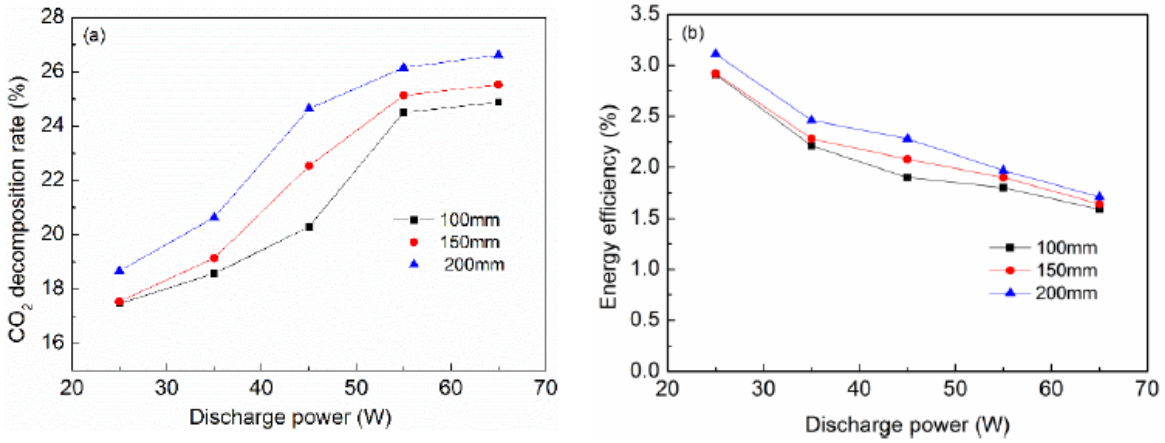

Figure 20: CO_2 decomposition rate and energy efficiency in the reactor at different discharge power[70].

power is necessary for a viewpoint of energy saving. Taking into account the discharge power of 55 W, the CO_2 decomposition rate in unpacked reactor is 26.1%, in the glass beads 33.5% and with ZrO_2 reach 52.1%. At the same time the energy efficiency only in ZrO_2 pellets improve by a factor of two. This can be explained by different factor such as the filling material in the discharge zone that made a more stable and stronger discharge zone; by the electric field enhancement due to the polarization of the dielectric material and by the strengthening of the electric field near the contact points of the pellets, causing a enhancement of the electron temperature and hence a positive effect on the CO_2 decomposition[38]. Finally the ZrO_2 as can be seen from all the result exhibit a better reaction activity than the glass beads, this is probably due to the fast oxygen ions migration[74]. The last configuration is made by ZrO_2-CeO_2 grinding balls(75% ZrO_2 and 25% CeO_2) of various diameter (from 1.0 mm to 2.0 mm)[47]. In this analysis different parameter have been changed such as: discharge power, feed flow rate and particle size. The first effect can be seen in fig.22 where the CO_2 conversion and energy efficiency are presented as a function of discharge power and feed flow rate. The maximum conversion reached is 64.3% at 110 W and 20 mL/min, while the maximum energy efficiency equal to 8.7% have been obtained when the the power was 30 W and feed flow rate equal to 100 mL/min. So by increasing the discharge power, a positive effect is obtained also for the conversion of the CO_2. Thus can be explained by the higher electric field that enhance the amount of high energy particle, this leads to more chemical reaction channel for the CO_2 conversion[64]. As regards the flow rate, it can be seen that lowering the feed flow rate, the conversion increase, this is due to the higher residence time which create more

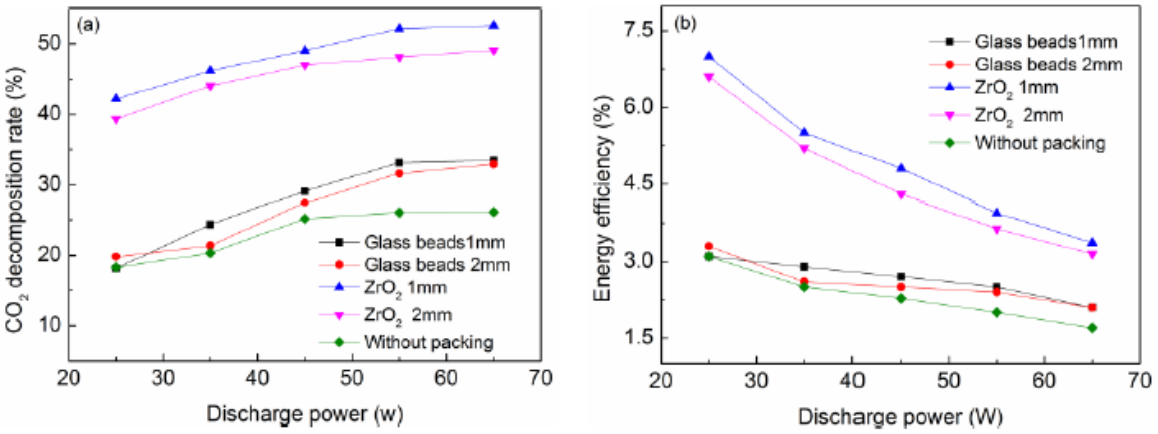

Figure 21: CO_2 decomposition rate and energy efficiency using different packing bed sized at different discharge power [70].

opportunities to participate in the reaction. On the contrary, the energy efficiency has the opposite trend, it decrease when the power increased and decreased when the flow rate decreased. More suitable packing materials are under investigation to enhance both this terms[47]. A better illustration of the conversion and the energy efficiency can be seen

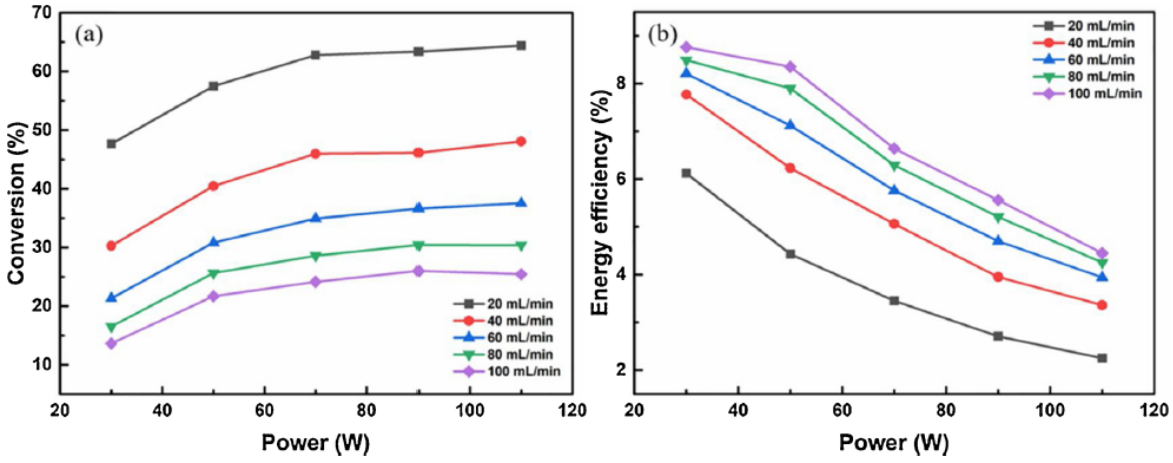

Figure 22: Effects of discharge power and feed flow rate on CO_2 conversion and energy efficiency[47]

in fig.23. In particular in the fig.23(a) the plasma power increase from 30 W to 110 W, while the feed flow rate was fixed at 20 mL/min, while in fig.23(b) the discharge power is fixed at 70 W, and the flow rate change from 20 mL/min to 100 mL/min. Obviously the effect are different in the two configuration and the results obtained in term of conversion and efficiency are closely related to the residence time which occurs. These means that the control of the feed flow rate is more immediate and more efficient than the changing

of the discharge power[47]. Last effect under investigation was the particles size, as can

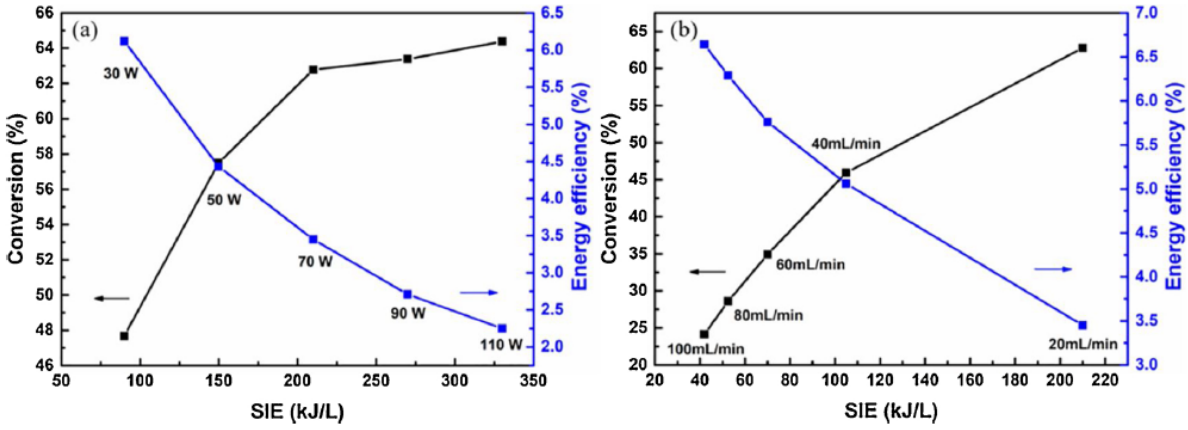

Figure 23: Effects of discharge power or feed flow rate and SIE on CO_2 conversion and energy efficiency[47]

be seen from fig.24, that vary from 1.0-1.2 mm, 1.4-1.6 mm and 1.8-2.0 mm. If the same packing volume is used, by decreasing the particle size, the number of the packing particle increase and this increase the contact point between the particle them self. In this way, by decreasing the particle size, more CeO_2 can be filled in the reactor that enable more oxygen absorption to block the reverse reaction. Then, more particle means to have more contact points of reactions that create a more uniform discharge over all the reactor and reach an higher conversion[45]. The implementation of a catalysis composed by ZrO_2-

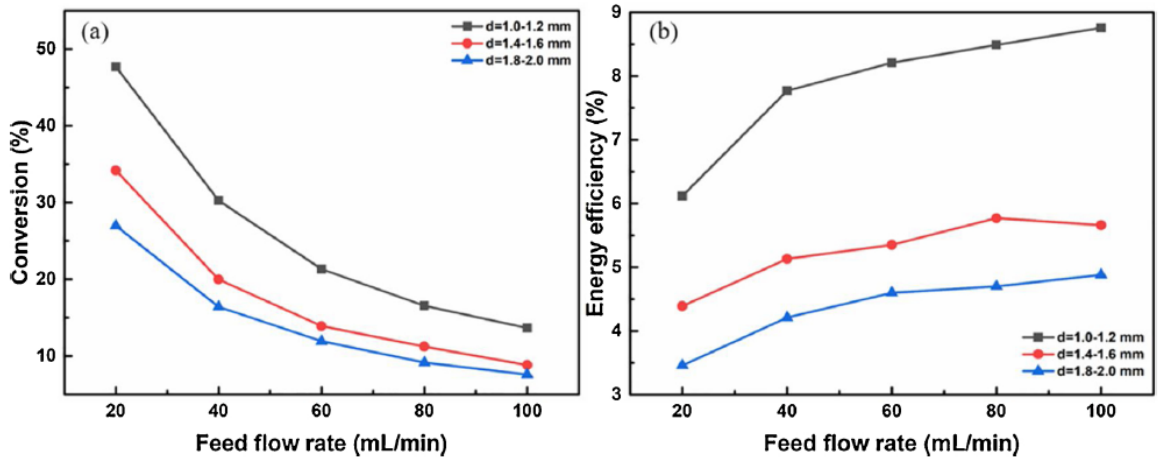

Figure 24: Effects of particle size on CO_2 conversion and energy efficiency[47]

CeO_2 have shown better proprieties than all the other type of catalytic material, reaching a maximum conversion of 64.38% and an energy efficiency of 8.76% which are the highest in the literature nowadays[47].

3 Experimental setup

An overview of the primary workbench is represented in the below figures. Where at first a general overview is depicted (fig.25) and then a more detailed image referring the plasma source (fig.26).

Figure 25: Overall view od the workbench

Then additional element that are part of the workbench are the generator FG5001 (fig.27) and the power unit control (fig.28). Optical Emission Spectroscopy (OES) is an analytical technique used to study the chemical and physical species present in a plasma, particularly to identify and quantify the atoms, ions, and molecules emitted during the electronic excitation process. When species in the plasma are excited by an electric field or by collisions with high-energy electrons, they absorb energy and reach high-energy states. Upon returning to a lower energy state, these species emit electromagnetic radiation in the form of visible or ultraviolet light, which can be analyzed to determine their composition [31]. Emission spectroscopy is based on measuring the wavelengths of light emitted by the excited species. Each chemical element and ion emit light at characteristic wavelengths, allowing for the identification of specific components in the plasma. The obtained emission lines also provide information about the electron temperature of the plasma, as the distribution of the intensity of spectral lines is strongly influenced by temperature. One of the main applications of optical emission spectroscopy in plasma research is the

Figure 26: Plasma Source (Openair-Plasma PFW10) and Optical probe

Figure 27: Generator FG5001

Figure 28: Power control Unit (range from 400 W to 600 W)

analysis of atomic and ionic species, providing critical information on electron density and plasma chemical composition [75]. In particular, the intensity of emission lines from ions such as O^+, Ar^+, or $N_2{}^+$ can be correlated with ion density and electron temperature in the plasma. Additionally, OES is useful for analyzing chemical processes and reactions that occur within the plasma, such as ionization, dissociation, and recombination.* In our experimental work on CO_2 conversion to CO and O, optical emission spectroscopy played a key role in identifying and monitoring the chemical species involved in this process. Plasma was used to dissociate the CO_2 molecule into carbon monoxide (CO) and oxygen (O) through processes such as auto-ionization and collision-induced dissociation. The formation of excited species like O^*, CO^*, and $O_2{}^*$, which emit light at different wavelengths, was tracked and analyzed to better understand the dynamics of this reaction. By measuring the intensity of the emission lines of these species, we were able to obtain information on the effects of the applied electrical parameters and the reaction conditions within the plasma. Such information can help optimize CO_2 conversion processes. Therefore, optical emission spectroscopy not only provides data on the composition of the involved species but also offers important details on the kinetics of the chemical reactions occurring in the plasma during CO_2 reduction. In our experiments, the parameters that are typically modified to assess the variation in terms of conversion efficiency are: the electric voltage, the frequency, and the amount of gas (CO_2) fed into the plasma source. The accuracy of the measurements depends on several factors, including the calibration of the spectrometer, interference from overlapping spectral lines, and the presence of self-absorption effects. To obtain quantitative data, it is often necessary to perform measurements under well-controlled conditions and to use calibration methods based on known reference sources. Despite the challenges and difficulties encountered, optical emission spectroscopy has been the most effective tool we have employed to study plasma-chemical characteristics, for real-time monitoring, and to track the evolution of species as a function of various parameters. An Ocean Optics LIBS2500 Plus spectrometer (Ocean Optics, Inc., Dunedin, FL, USA), a fiber optic cable and the OceanView computer software (OceanView version 2.0.8) were used to examine the spectra of the species in the sensitive range from 150 to 1100 nm as wavelength (fig.29). The probe was placed near the plasma jet to operate in an overpressure environment. This setup allows for the assessment of the plasma flow's capacity without interference from the surrounding air in the treatment chamber. The OES reveals the ionizing potential of the chemical species involved and their variations in response to the primary plasma parameters. This information offers valuable initial guidance for selecting the appropriate parameters to combine with preliminary experiments.

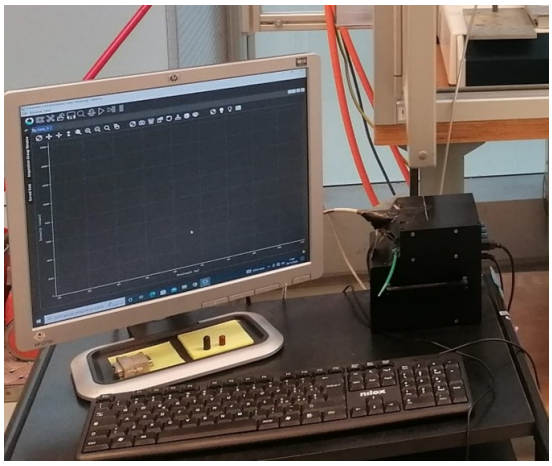

Figure 29: Screen displaying spectra acquired in real time and OES analyser

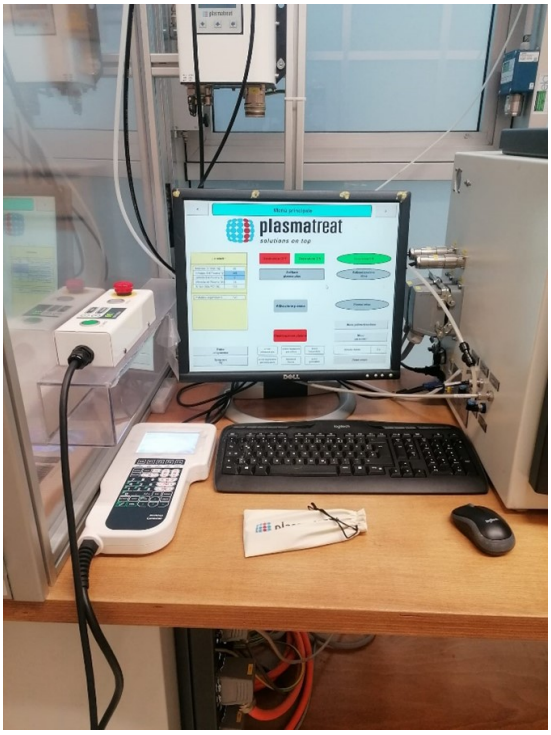

Figure 30: Process parameter display screen and control panel

4 Test Pure CO_2

A primary test has been performed with the aim to investigate the different species that are obtained when the splitting occurs. In that case the main purpose is to verify the different conditions that the plasma torch is able to sustain. Indeed, the plasma torch has a limited application on this field, and as explained before other type of plasma are preferred in this type of application. In the following case the gas is composed by pure CO_2 with a flow rate equal to 40 L/min, frequency equal to 25 kHz and operate at maximum power. These parameters have been founded after different experimental analysis due to the impossibility of the plasma to remain continuously active. As a matter of fact the most critical parameter has been the power of the plasma torch. If the value imposed was not the maximum one, the plasma could not be formed. This is probably due to the amount of energy transferred to the pure CO_2 gas flow which is not sufficient to split the molecules and the lack of energy is manifested in this phenomena. Apart of that, the gas flow rate can be managed and imposed with a different value than the one selected. In that experiment, another important parameter has been analyzed which is the nozzle of

the plasma torch. Several nozzles have been tested to figured out which is the best one in terms of output intensity of the created species. The results obtained during the testing of all the nozzles lead to the possibility of using only of two of them, the nozzle with laboratory number "31445" and "36002-03". The incapacity of using all the other nozzles is because the plasma cannot be activated with the fixed parameter previously described. While, only those nozzle could sustain the plasma and making the effective splitting of the CO_2. The result obtained from the two experiment can be seen thanks the OES and then plotted in the wavelength number and relative intensity graph.

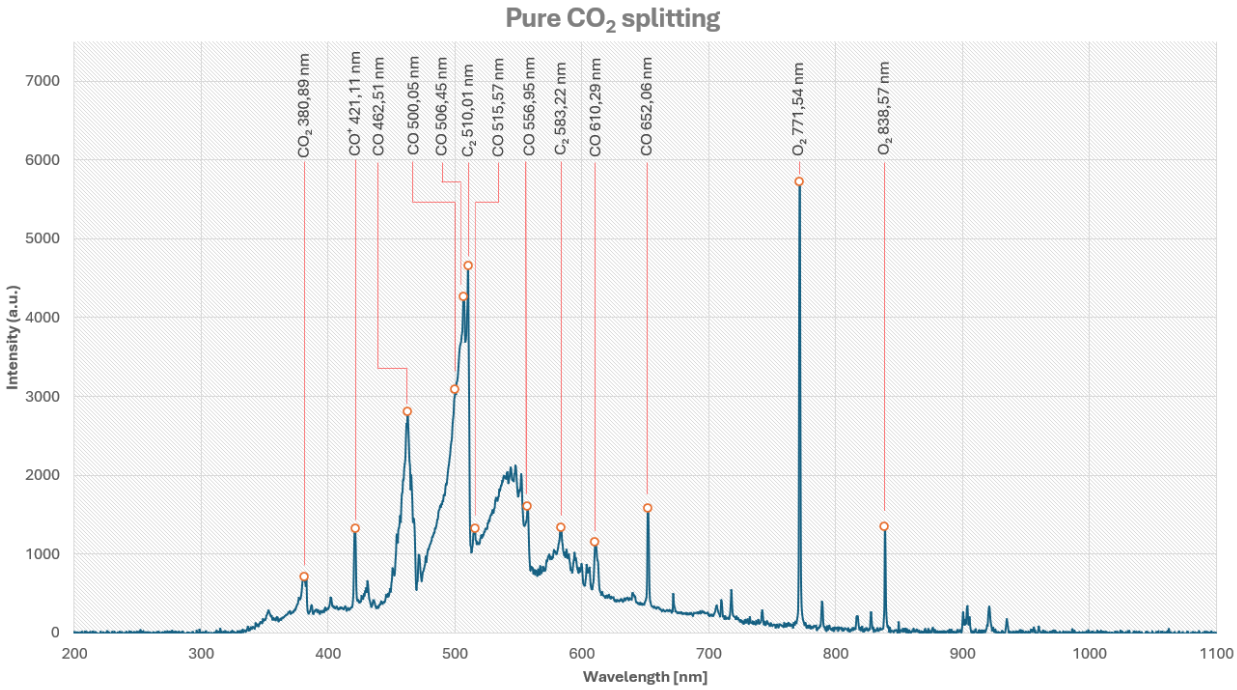

Figure 31: Pure CO_2 spectrum with nozzle 31445

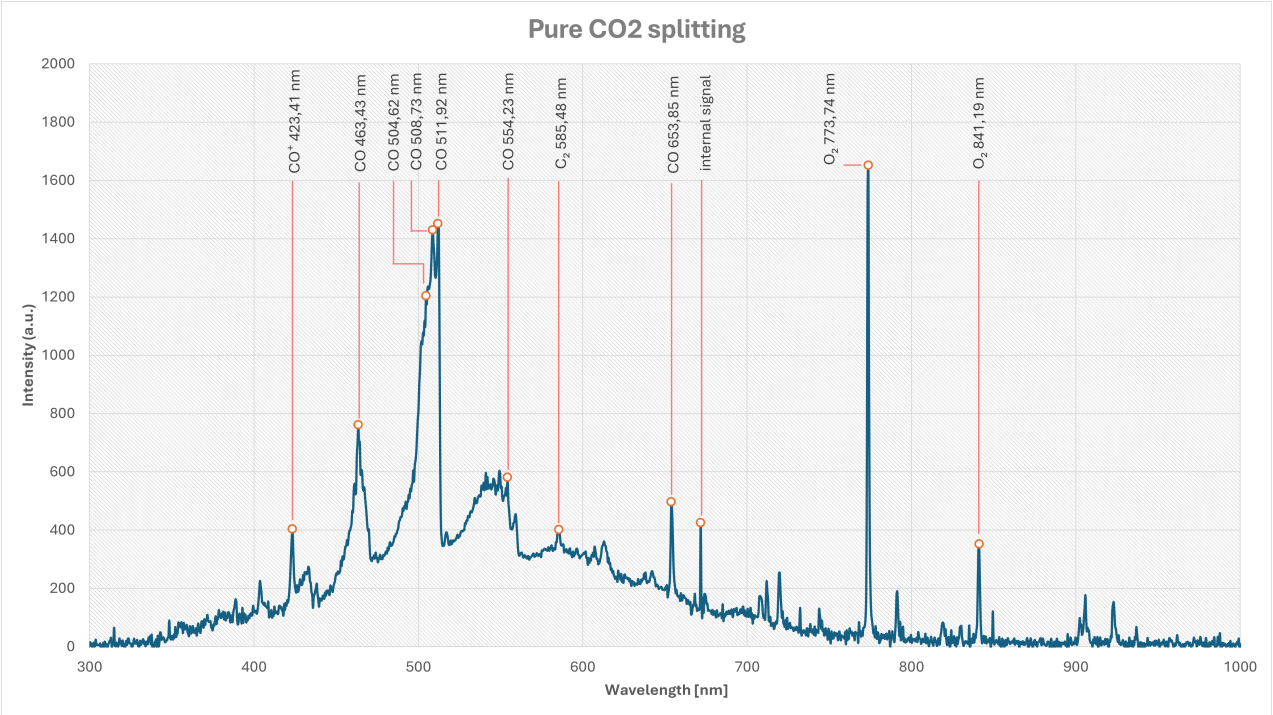

Figure 32: Pure CO_2 spectrum with nozzle 36002-03

Once that the species were formed and plotted into the graph fig.31 and fig.32, a more deepest analysis has been made in order to identify the exact species that correspond to each peaks. First of all, a main different between the two nozzle is the intensity of the peaks that are reached. Actually, with the "31445" an intensity of almost 6000 is reached, while for the "36002-03" the value is neither 1700. This means that the created species are better recognized with the first nozzle. Nevertheless, having an higher intensity, the peaks of the former nozzle are more simple to recognize, while the latter having also a background noise it makes more difficult to identify the more important species. The peak with the highest intensity is the most simple to recognize and is refereed to the presence of O_2 that always have a wavelength equal to 777.5 nm and 838.5 nm in both the case under examination [76]. Starting with the first nozzle, the other peaks are refereed to the presence of the CO_2, the splitting of this molecule generates other compounds like CO, C_2 and CO^+. To better understand which peak identify each species, a further investigation has been made by looking at each wavelength and identify all the single species. Starting with the presence of CO_2 in the spectrum means that not all the feed gas have been converted in the other products. That is not a negative sign, but simply indicate that in those operating conditions the amount of pure CO_2 cannot be split at all. Nevertheless, the band spectrum of the pure CO_2 is in the wavelength range of 300-400 nm with a strong peak at 380,89 nm that represent the strongest CO_2 sign in our case. Moving

to the formation of the CO and CO^+, the band in which this two species are present is pretty wide, however some peak correspondences are present into some wavelength point. In particular for the $CO\hat{+}$ the peak at 421,11 nm correspond to the "Comet-tail system" with an high intensity[76]. Regarding the CO, the first peak that correspond to 462.51 nm is correlated to the "Carbon monoxide flame spectrum"[76]. Then the next peaks are represented of the so called "Triplet bands zone" in which three consecutive point close to each other with a relative high peak[76]. Finally all the remaining peaks that are related to the CO and accounted together in the "Angstrom band system"[76]. In the spectrum are also present peaks that belong to the "Swan system" corresponding to the wavelength 510.10 nm and 583.22 nm. Those ones depicts the presence of the molecule C_2 which are present due to the recombination of the carbon atoms[76]. A summary of all the wavelength and the species founded in the case of gas feed by pure CO_2 with the "31445" nozzle are showed at Table 1.

Wavelength (λ) [nm]	**Species**
380.89	CO_2
421.11	CO^+
462.51	CO
500.05	CO
506.45	CO
510.10	C_2
515.57	CO
556.95	CO
583.22	C_2
610.29	CO
652.06	CO
771.54	O_2
838.57	O_2

Table 1: Table with wavelength number and corresponding species with nozzle 31445

Wavelength (λ) [nm]	**Species**
423.41	CO^+
463.43	CO
504.62	CO
508.73	CO
511.92	CO
554.23	CO
585.48	C_2
653.85	CO
671.74	Internal signal
773.74	O_2
841.19	O_2

Table 2: Table with wavelength number and corresponding species with nozzle 36002-03

As previously said, the second experiment made with the nozzle "36002-03" reach a lower intensity in terms of peak and to identify the exact species could have been more difficult. Firstly, the lower intensity of the peaks can be caused by the material of the nozzle itself. This can interact with the exiting species from the plasma torch and make the measurement from the OES less readable. However, most of the species were the same of the nozzle "31445". In that case the peak representing the CO_2 in the range 300-400 nm is not present, that means that all the flow rate feeding the system has been converted or has not been detected from the OES. Nevertheless, as can be seen from the result reported in the Table 2, peaks representing the CO^+ and CO have been detected. Respectively the CO^+ wavelength at 423.41 nm is representing of the "Comet-tail system" [76] while the CO at 463.43 nm and 554.23 nm are identified respectively in the "Carbon monoxide flame spectrum"[76] and "Angstrom band system"[76]. Better than the previous nozzle can be seen the three peaks of CO at 504.62 nm, 508.73 nm and 511.92 nm representing the "Triplet bands zone" [76]. Finally the presence of a mechanism of recombination is depicted by the presence of the "Swan system" with the peak at 585.48 nm [76].

5 Conclusion

The continuous increasing of emission of the CO_2 leads to new solution for the reduction of carbon in the atmosphere. The potential of using a system like plasma with the advantage to produce useful product has become really interesting and attractive in the recent years. Despite mostly of the research are concentrated in the using of DBD plasma, the evaluation of using other type of plasma, like plasma torch could have a significant role in the future. In that review an illustration of the current main technologies have been reported. The most interesting thing is that with different plasma configuration the value of efficiency and CO_2 conversion can be almost the same. For each typology of plasma, further analysis has been made in order to find the most appropriate criteria to have the maximum conversion. Thus can be obtained by several measurement and vary some important parameters such as flow rate, pressure, inert gasses, frequency, discharge power and catalytic material. The catalytic material, in particular, have a crucial role because is able to enhance the conversion and the efficiency much higher than the other metrics. The most effective results are obtained with CeO_2 and ZrO_2, that could be present in the catalytic material alone or combined together to take advantage of both proprieties. Nevertheless, the addition of an inert gas like N_2 and Ar leads to a much higher CO_2 conversion. Thus, combined together with the catalytic material could result in the best configuration for the plasma torch in terms of efficiency and CO_2 conversion.

List of Figure

List of Table

References

[1] A. Ozkan, *CO 2 splitting in a dielectric barrier discharge plasma: Understanding of physical and chemical aspects*, 2016.

[2] R. Snoeckx and A. Bogaerts, "Plasma technology – a novel solution for CO $_2$ conversion?" *Chemical Society Reviews*, vol. 46, no. 19, pp. 5805–5863, 2017, ISSN: 0306-0012, 1460-4744. DOI: 10.1039/C6CS00066E.

[3] G. Chen, L. Wang, T. Godfroid, and R. Snyders, "Progress in plasma-assisted catalysis for carbon dioxide reduction," in *Plasma Chemistry and Gas Conversion*, N. Britun and T. Silva, Eds., Rijeka: IntechOpen, 2018, ch. 4. DOI: 10.5772/intechopen.80798.

[4] H. Puliyalil, D. L. Jurković, V. D. B. C. Dasireddy, and B. Likozar, *A review of plasma-assisted catalytic conversion of gaseous carbon dioxide and methane into value-added platform chemicals and fuels*, Royal Society of Chemistry, 2018. DOI: 10.1039/c8ra03146k.

[5] H. J. Gallon, H.-H. Kim, X. Tu, and J. C. Whitehead, "Microscope–ICCD Imaging of an Atmospheric Pressure $\hbox{CH}_{4}$ and $\hbox{CO}_{2}$ Dielectric Barrier Discharge," *IEEE Transactions on Plasma Science*, vol. 39, no. 11, pp. 2176–2177, Nov. 2011, ISSN: 0093-3813, 1939-9375. DOI: 10.1109/TPS.2011.2157946.

[6] U. Kogelschatz, *Dielectric-Barrier Discharges: Their History, Discharge Physics, and Industrial Applications.*

[7] A. Fridman, A. Chirokov, and A. Gutsol, "Non-thermal atmospheric pressure discharges," *Journal of Physics D: Applied Physics*, vol. 38, no. 2, R1–R24, Jan. 21, 2005, ISSN: 0022-3727, 1361-6463. DOI: 10.1088/0022-3727/38/2/R01.

[8] Y. Vadikkeettil, Y. Subramaniam, R. Murugan, *et al.*, "Plasma assisted decomposition and reforming of greenhouse gases: A review of current status and emerging trends," *Renewable and Sustainable Energy Reviews*, vol. 161, p. 112 343, Jun. 2022, ISSN: 13640321. DOI: 10.1016/j.rser.2022.112343.

[9] Y. Yin, T. Yang, Z. Li, E. Devid, D. Auerbach, and A. W. Kleyn, "CO $_2$ conversion by plasma: How to get efficient CO $_2$ conversion and high energy efficiency," *Physical Chemistry Chemical Physics*, vol. 23, no. 13, pp. 7974–7987, 2021, ISSN: 1463-9076, 1463-9084. DOI: 10.1039/D0CP05275B.

[10] X. Ma, S. Li, M. Ronda-Lloret, *et al.*, "Plasma Assisted Catalytic Conversion of CO2 and H2O Over Ni/Al2O3 in a DBD Reactor," *Plasma Chemistry and Plasma Processing*, vol. 39, no. 1, pp. 109–124, Jan. 2019, ISSN: 0272-4324, 1572-8986. DOI: 10.1007/s11090-018-9931-1.

[11] A. George, B. Shen, M. Craven, *et al.*, "A Review of Non-Thermal Plasma Technology: A novel solution for CO2 conversion and utilization," *Renewable and Sustainable Energy Reviews*, vol. 135, p. 109 702, Jan. 2021, ISSN: 13640321. DOI: 10.1016/j.rser.2020.109702.

[12] L. Yu, X. Li, X. Tu, Y. Wang, S. Lu, and J. Yan, "Decomposition of naphthalene by dc gliding arc gas discharge," *The Journal of Physical Chemistry A*, vol. 114, no. 1, pp. 360–368, 2010. DOI: 10.1021/jp905082s.

[13] P. V. M. Alves, S. C. Pinto, A. P. Serro, and M. I. Gil, "Surface modification of a thermoplastic polyurethane by low-pressure plasma treatment to improve hydrophilicity," *Journal of Applied Polymer Science*, vol. 122, no. 4, pp. 2302–2308, Jun. 2011. DOI: 10.1002/app.34348. [Online]. Available: https://doi.org/10.1002/app.34348.

[14] A. V. Nastuta, I. Topala, C. Grigoras, V. Pohoata, and G. Popa, "Stimulation of wound healing by helium atmospheric pressure plasma treatment," *Journal of Physics D: Applied Physics*, vol. 44, no. 10, p. 105 204, Mar. 16, 2011, ISSN: 0022-3727, 1361-6463. DOI: 10.1088/0022-3727/44/10/105204.

[15] A. Schutze, J. Jeong, S. Babayan, Jaeyoung Park, G. Selwyn, and R. Hicks, "The atmospheric-pressure plasma jet: A review and comparison to other plasma sources," *IEEE Transactions on Plasma Science*, vol. 26, no. 6, pp. 1685–1694, Dec./1998, ISSN: 00933813. DOI: 10.1109/27.747887.

[16] S. Bekeschus, A. Schmidt, K.-D. Weltmann, and T. Von Woedtke, "The plasma jet kINPen – A powerful tool for wound healing," *Clinical Plasma Medicine*, vol. 4, no. 1, pp. 19–28, Jul. 2016, ISSN: 22128166. DOI: 10.1016/j.cpme.2016.01.001.

[17] E. C. Neyts, K. (Ostrikov, M. K. Sunkara, and A. Bogaerts, "Plasma catalysis: Synergistic effects at the nanoscale," *Chemical Reviews*, vol. 115, no. 24, pp. 13 408–13 446, 2015, PMID: 26619209. DOI: 10.1021/acs.chemrev.5b00362.

[18] S. Rayne, "Carbon dioxide splitting: A summary of the peer-reviewed scientific literature," *Nature Precedings*, Apr. 2008. DOI: 10.1038/npre.2008.1741.1.

[19] Z. Jiang, T. Xiao, V. Kuznetsov, and P. Edwards, "Turning carbon dioxide into fuel," *Philosophical transactions. Series A, Mathematical, physical, and engineering sciences*, vol. 368, pp. 3343–64, Jul. 2010. DOI: 10.1098/rsta.2010.0119.

[20] D. Wagman, J. Kilpatrick, W. Taylor, K. Pitzer, and F. Rossini, "Heats, free energies, and equilibrium constants of some reactions involving O2, H2, H2O, C, CO, CO2, and CH4," *Journal of Research of the National Bureau of Standards*, vol. 34, no. 2, p. 143, Feb. 1945, ISSN: 0091-0635. DOI: 10.6028/jres.034.004.

[21] A. Fridman, *Plasma Chemistry I.* Jan. 2008, ISBN: 9780521847353. DOI: 10.1017/CBO9780511546075.

[22] A. Bogaerts, A. Berthelot, S. Heijkers, *et al.*, "Co2 conversion by plasma technology: Insights from modeling the plasma chemistry and plasma reactor design," *Plasma Sources Science and Technology*, vol. 26, no. 6, p. 063 001, May 2017. DOI: 10.1088/1361-6595/aa6ada. [Online]. Available: https://dx.doi.org/10.1088/1361-6595/aa6ada.

[23] R. I. Azizov, A. K. Vakar, V. K. Zhivotov, *et al.*, "Nonequilibrium plasmachemical process of CO2 decomposition in a supersonic microwave discharge," *Akademiia Nauk SSSR Doklady*, vol. 271, pp. 94–98, Aug. 1983.

[24] I. Belov, V. Vermeiren, S. Paulussen, and A. Bogaerts, "Carbon dioxide dissociation in a microwave plasma reactor operating in a wide pressure range and different gas inlet configurations," *Journal of CO2 Utilization*, vol. 24, pp. 386–397, 2018, ISSN: 2212-9820. DOI: https://doi.org/10.1016/j.jcou.2017.12.009.

[25] M. Ong, S. Nomanbhay, F. Kusumo, and P. Show, "Application of microwave plasma technology to convert carbon dioxide (co2) into high value products: A review," *Journal of Cleaner Production*, vol. 336, p. 130 447, 2022, ISSN: 0959-6526. DOI: https://doi.org/10.1016/j.jclepro.2022.130447.

[26] N. Britun, T. Silva, G. Chen, T. Godfroid, J. van der Mullen, and R. Snyders, "Plasma-assisted co2 conversion: Optimizing performance via microwave power modulation," *Journal of Physics D: Applied Physics*, vol. 51, no. 14, p. 144 002, Mar. 2018. DOI: 10.1088/1361-6463/aab1ad. [Online]. Available: https://dx.doi.org/10.1088/1361-6463/aab1ad.

[27] D. Czylkowski, B. Hrycak, M. Jasiński, M. Dors, and J. Mizeraczyk, "Microwave plasma-based method of hydrogen production via combined steam reforming of

methane," *Energy*, vol. 113, pp. 653–661, 2016, ISSN: 0360-5442. DOI: https://doi.org/10.1016/j.energy.2016.07.088.

[28] N. Lu, C. Zhang, K. Shang, N. Jiang, J. Li, and Y. Wu, "Corrigendum: Dielectric barrier discharge plasma assisted co2 conversion: Understanding the effects of reactor design and operating parameters (2019 j. phys. d: Appl. phys. 52 224003)," *Journal of Physics D: Applied Physics*, vol. 52, no. 31, p. 319 501, May 2019. DOI: 10.1088/1361-6463/ab2171.

[29] L. Li, H. Zhang, X. Li, *et al.*, "Plasma-assisted co2 conversion in a gliding arc discharge: Improving performance by optimizing the reactor design," *Journal of CO2 Utilization*, vol. 29, pp. 296–303, 2019, ISSN: 2212-9820. DOI: https://doi.org/10.1016/j.jcou.2018.12.019.

[30] S. Mohsenian, D. Nagassou, R. Elahi, *et al.*, "Carbon dioxide conversion by solar-enhanced microwave plasma: Effect of specific power and argon/nitrogen carrier gases," *Journal of CO2 Utilization*, vol. 34, pp. 725–732, 2019, ISSN: 2212-9820. DOI: https://doi.org/10.1016/j.jcou.2019.09.002.

[31] P. Navascués, J. Cotrino, A. R. González-Elipe, and A. Gómez-Ramírez, "Plasma assisted co2 dissociation in pure and gas mixture streams with a ferroelectric packed-bed reactor in ambient conditions," *Chemical Engineering Journal*, vol. 430, p. 133 066, 2022, ISSN: 1385-8947. DOI: https://doi.org/10.1016/j.cej.2021.133066.

[32] M. Ramakers, I. Michielsen, R. Aerts, V. Meynen, and A. Bogaerts, "Effect of argon or helium on the co2 conversion in a dielectric barrier discharge," *Plasma Processes and Polymers*, vol. 12, no. 8, pp. 755–763, 2015. DOI: https://doi.org/10.1002/ppap.201400213.

[33] S. Heijkers, R. Snoeckx, T. Kozák, *et al.*, "Co2 conversion in a microwave plasma reactor in the presence of n2: Elucidating the role of vibrational levels," *The Journal of Physical Chemistry C*, vol. 119, no. 23, pp. 12 815–12 828, 2015. DOI: 10.1021/acs.jpcc.5b01466.

[34] S. Paulussen, B. Verheyde, X. Tu, *et al.*, "Conversion of carbon dioxide to value-added chemicals in atmospheric pressure dielectric barrier discharges," *Plasma Sources Science and Technology*, vol. 19, pp. 34 015–6, Jun. 2010. DOI: 10.1088/0963-0252/19/3/034015.

[35] M. Schiorlin, R. Klink, and R. Brandenburg, "Carbon dioxide conversion by means of coplanar dielectric barrier discharges," *The European Physical Journal Applied Physics*, vol. 75, p. 24 704, Aug. 2016. DOI: 10.1051/epjap/2016160073.

[36] R. Aerts, W. Somers, and A. Bogaerts, "Carbon Dioxide Splitting in a Dielectric Barrier Discharge Plasma: A Combined Experimental and Computational Study," *ChemSusChem*, vol. 8, no. 4, pp. 702–716, Feb. 2015, ISSN: 1864-5631, 1864-564X. DOI: 10.1002/cssc.201402818.

[37] Q. Yu, M. Kong, T. Liu, J.-h. Fei, and X. Zheng, "Characteristics of the decomposition of co2 in a dielectric packed-bed plasma reactor," *Plasma Chemistry and Plasma Processing*, vol. 32, pp. 153–163, 2012. [Online]. Available: https://api.semanticscholar.org/CorpusID:95234918.

[38] A. Ozkan, A. Bogaerts, and F. Reniers, "Routes to increase the conversion and the energy efficiency in the splitting of co 2 by a dielectric barrier discharge," *Journal of Physics D: Applied Physics*, vol. 50, p. 084 004, Jan. 2017. DOI: 10.1088/1361-6463/aa562c.

[39] D. Mei and X. Tu, "Atmospheric Pressure Non-Thermal Plasma Activation of CO $_2$ in a Packed-Bed Dielectric Barrier Discharge Reactor," *ChemPhysChem*, vol. 18, no. 22, pp. 3253–3259, Nov. 17, 2017, ISSN: 1439-4235, 1439-7641. DOI: 10.1002/cphc.201700752.

[40] "Co2 decomposition using glow discharge plasmas," *Journal of Catalysis*, vol. 185, no. 1, pp. 152–159, 1999, ISSN: 0021-9517. DOI: https://doi.org/10.1006/jcat.1999.2499.

[41] R. Snoeckx, S. Heijkers, K. Van Wesenbeeck, S. Lenaerts, and A. Bogaerts, "Co2 conversion in a dielectric barrier discharge plasma: N2 in the mix as helping hand or problematic impurity?" *Energy Environmental Science*, vol. 9, pp. 999–1011, Mar. 2016. DOI: 10.1039/C5EE03304G.

[42] Q. Yu, M. Kong, T. Liu, J. Fei, and X. Zheng, "Characteristics of the Decomposition of CO2 in a Dielectric Packed-Bed Plasma Reactor," *Plasma Chemistry and Plasma Processing*, vol. 32, no. 1, pp. 153–163, Feb. 2012, ISSN: 0272-4324, 1572-8986. DOI: 10.1007/s11090-011-9335-y.

[43] I. Michielsen, Y. Uytdenhouwen, J. Pype, *et al.*, "Co2 dissociation in a packed bed dbd reactor: First steps towards a better understanding of plasma catalysis,"

English, *Chemical Engineering Journal*, vol. 326, no. C, pp. 477–488, 2017. DOI: 10.1016/j.cej.2017.05.177.

[44] K. Van Laer and A. Bogaerts, "Improving the conversion and energy efficiency of carbon dioxide splitting in a zirconia-packed dielectric barrier discharge reactor," *Energy Technology*, vol. 3, no. 10, pp. 1038–1044, 2015. DOI: https://doi.org/10.1002/ente.201500127.

[45] T. Butterworth, "Effects of particle size on co2 reduction and discharge characteristics in a packed bed plasma reactor," *The Chemical Engineering Journal*, vol. 293, Feb. 2016. DOI: 10.1016/j.cej.2016.02.047.

[46] X. Duan, Z. Hu, Y. Li, and B. Wang, "Effect of dielectric packing materials on the decomposition of carbon dioxide using dbd microplasma reactor," *AIChE Journal*, vol. 61, no. 3, pp. 898–903, 2015. DOI: https://doi.org/10.1002/aic.14682.

[47] "Co2 conversion in a coaxial dielectric barrier discharge plasma reactor in the presence of mixed zro2-ceo2," *Journal of Environmental Chemical Engineering*, vol. 9, no. 1, p. 104 654, 2021, ISSN: 2213-3437. DOI: https://doi.org/10.1016/j.jece.2020.104654.

[48] V. D. Rusanov, A. A. Fridman, and G. V. Sholin, "The physics of a chemically active plasma with nonequilibrium vibrational excitation of molecules,"

[49] T. Kozák and A. Bogaerts, "Splitting of co2 by vibrational excitation in nonequilibrium plasmas: A reaction kinetics model," *Plasma Sources Science and Technology*, vol. 23, p. 045 004, Jun. 2014. DOI: 10.1088/0963-0252/23/4/045004.

[50] G. J. van Rooij, D. C. M. van den Bekerom, N. den Harder, *et al.*, "Taming microwave plasma to beat thermodynamics in co2 dissociation," *Faraday Discuss.*, vol. 183, pp. 233–248, 0 2015. DOI: 10.1039/C5FD00045A.

[51] L. SpencerAlec and A. Gallimore, "Efficiency of co 2 dissociation in a radio-frequency discharge," *Plasma Chemistry and Plasma Processing - PLASMA CHEM PLASMA PROCESS*, vol. 31, pp. 79–89, Feb. 2011. DOI: 10.1007/s11090-010-9273-0.

[52] A. Vesel, M. Mozetic, A. Drenik, and M. Balat-Pichelin, "Dissociation of co 2 molecules in microwave plasma," *Chemical Physics - CHEM PHYS*, vol. 382, pp. 127–131, Apr. 2011. DOI: 10.1016/j.chemphys.2011.03.015.

[53] L. F. Spencer and A. D. Gallimore, "Co2 dissociation in an atmospheric pressure plasma/catalyst system: A study of efficiency," *Plasma Sources Science and Technology*, vol. 22, no. 1, p. 015 019, Dec. 2012. DOI: 10.1088/0963-0252/22/1/015019. [Online]. Available: https://dx.doi.org/10.1088/0963-0252/22/1/015019.

[54] M. Tsuji, T. Tanoue, K. Nakano, and Y. Nishimura, "Decomposition of CO2 into CO and O in a Microwave-Excited Discharge Flow of CO2/He or CO2/Ar Mixtures," *Chemistry Letters*, vol. 30, no. 1, pp. 22–23, Aug. 2002.

[55] G. Chen, N. Britun, T. Godfroid, M. Delplancke, and R. Snyders, "Role of plasma catalysis in the microwave plasma-assisted conversion of co2," Jul. 2017. DOI: 10.5772/67874.

[56] T. Nunnally, K. Gutsol, A. Rabinovich, A. Fridman, A. Gutsol, and A. Kemoun, "Dissociation of co2 in a low current gliding arc plasmatron," *Journal of Physics D: Applied Physics*, vol. 44, no. 27, p. 274 009, Jun. 2011. DOI: 10.1088/0022-3727/44/27/274009. [Online]. Available: https://dx.doi.org/10.1088/0022-3727/44/27/274009.

[57] I. Rusu and J.-M. Cormier, "On a possible mechanism of the methane steam reforming in a gliding arc reactor," *Chemical Engineering Journal*, vol. 91, no. 1, pp. 23–31, 2003.

[58] S. Sun, H. Wang, D. Mei, X. Tu, and A. Bogaerts, "Co2 conversion in a gliding arc plasma: Performance improvement based on chemical reaction modeling," *Journal of CO2 Utilization*, vol. 17, pp. 220–234, 2017, ISSN: 2212-9820. DOI: https://doi.org/10.1016/j.jcou.2016.12.009. [Online]. Available: https://www.sciencedirect.com/science/article/pii/S2212982016304206.

[59] G. Trenchev, S. Kolev, W. Wang, M. Ramakers, and A. Bogaerts, "Co2 conversion in a gliding arc plasmatron: Multidimensional modeling for improved efficiency," *The Journal of Physical Chemistry C*, vol. 121, no. 44, pp. 24 470–24 479, 2017. DOI: 10.1021/acs.jpcc.7b08511.

[60] A. Indarto, J.-W. Choi, H. Lee, and H. K. Song, "Conversion of co2 by gliding arc plasma," *Environmental Engineering Science*, vol. 23, no. 6, pp. 1033–1043, 2006. DOI: 10.1089/ees.2006.23.1033.

[61] E. C. Neyts, K. (Ostrikov, M. K. Sunkara, and A. Bogaerts, "Plasma catalysis: Synergistic effects at the nanoscale," *Chemical Reviews*, vol. 115, no. 24, pp. 13 408–13 446, 2015. DOI: 10.1021/acs.chemrev.5b00362.

[62] K. Neyts and F. Beunis, "Ion transport in liquid crystals," in *Handbook of Liquid Crystals*. John Wiley Sons, Ltd, 2014, ch. 11, pp. 1–26, ISBN: 9783527671403. DOI: https://doi.org/10.1002/9783527671403.hlc032.

[63] Z. Wang, Y. Zhang, E. C. Neyts, *et al.*, "Catalyst preparation with plasmas: How does it work?" *ACS Catalysis*, vol. 8, no. 3, pp. 2093–2110, 2018. DOI: 10.1021/acscatal.7b03723.

[64] L. Wang, Y. Zhao, C. Liu, W. Gong, and H. Guo, "Plasma driven ammonia decomposition on a fe-catalyst: Eliminating surface nitrogen poisoning," *Chem. Commun.*, vol. 49, pp. 3787–3789, 36 2013. DOI: 10.1039/C3CC41301B.

[65] X. Tu, H. J. Gallon, M. V. Twigg, P. A. Gorry, and J. C. Whitehead, "Dry reforming of methane over a ni/al2o3 catalyst in a coaxial dielectric barrier discharge reactor," *Journal of Physics D: Applied Physics*, vol. 44, no. 27, p. 274 007, Jun. 2011. DOI: 10.1088/0022-3727/44/27/274007. [Online]. Available: https://dx.doi.org/10.1088/0022-3727/44/27/274007.

[66] S. Gadkari, X. Tu, and S. Gu, "Fluid model for a partially packed dielectric barrier discharge plasma reactor," *Physics of Plasmas*, vol. 24, no. 9, p. 093 510, Aug. 2017. DOI: 10.1063/1.5000523. eprint: https://pubs.aip.org/aip/pop/article-pdf/doi/10.1063/1.5000523/15660305/093510_1_online.pdf. [Online]. Available: https://doi.org/10.1063/1.5000523.

[67] K. Van Laer and A. Bogaerts, "Influence of gap size and dielectric constant of the packing material on the plasma behaviour in a packed bed dbd reactor: A fluid modelling study," *Plasma Processes and Polymers*, vol. 14, Sep. 2016. DOI: 10.1002/ppap.201600129.

[68] H. Ji, L. Lin, and K. Chang, "Plasma-assisted co2 decomposition catalyzed by ceo2 of various morphologies," *Journal of CO2 Utilization*, vol. 68, p. 102 351, 2023, ISSN: 2212-9820. DOI: https://doi.org/10.1016/j.jcou.2022.102351.

[69] T. Sakpal and L. Lefferts, "Structure-dependent activity of ceo2 supported ru catalysts for co2 methanation," *Journal of Catalysis*, vol. 367, pp. 171–180, 2018, ISSN: 0021-9517. DOI: https://doi.org/10.1016/j.jcat.2018.08.027.

[70] A. Zhou, D. Chen, C. Ma, F. Yu, and B. Dai, "Dbd plasma-zro2 catalytic decomposition of co2 at low temperatures," *Catalysts*, vol. 8, no. 7, 2018, ISSN: 2073-4344. DOI: 10.3390/catal8070256.

[71] D. Mei, Y.-L. He, S. Liu, J. Yan, and X. Tu, "Optimization of co2 conversion in a cylindrical dielectric barrier discharge reactor using design of experiments," *Plasma Processes and Polymers*, vol. 13, no. 5, pp. 544–556, 2016. DOI: https://doi.org/10.1002/ppap.201500159.

[72] A. Zhou, D. Chen, B. Dai, C. Ma, P. Li, and F. Yu, "Direct decomposition of co2 using self-cooling dielectric barrier discharge plasma," *Greenhouse Gases: Science and Technology*, vol. 7, no. 4, pp. 721–730, 2017. DOI: https://doi.org/10.1002/ghg.1683.

[73] D. Mei, X. Zhu, Y.-L. He, J. D. Yan, and X. Tu, "Plasma-assisted conversion of co2 in a dielectric barrier discharge reactor: Understanding the effect of packing materials," *Plasma Sources Science and Technology*, vol. 24, no. 1, p. 015 011, Dec. 2014. DOI: 10.1088/0963-0252/24/1/015011.

[74] N. Mahato, A. Banerjee, A. Gupta, S. Omar, and K. Balani, "Progress in material selection for solid oxide fuel cell technology: A review," *Progress in Materials Science*, vol. 72, pp. 141–337, 2015, ISSN: 0079-6425. DOI: https://doi.org/10.1016/j.pmatsci.2015.01.001.

[75] T. Silva, N. Britun, T. Godfroid, and R. Snyders, "Understanding co2 decomposition in microwave plasma by means of optical diagnostics," *Plasma Processes and Polymers*, vol. 14, no. 6, p. 1 600 103, 2017. DOI: https://doi.org/10.1002/ppap.201600103.

[76] R. W. B. Pearse, A. G. Gaydon, R. W. B. Pearse, and A. G. Gaydon, *The identification of molecular spectra*. Chapman and Hall London, 1976, vol. 297.